1968

Solution of the space-time dependent neutron kinetics equations for a reflected slab reactor

James Hugh McFadden
Iowa State University

69-4258

McFADDEN, James Hugh, 1940-

SOLUTION OF THE SPACE-TIME DEPENDENT NEUTRON KINETICS EQUATIONS FOR A REFLECTED SLAB REACTOR.

Iowa State University, Ph.D., 1968
Engineering, nuclear

University Microfilms, Inc., Ann Arbor, Michigan

SOLUTION OF THE SPACE-TIME DEPENDENT NEUTRON KINETICS EQUATIONS FOR A REFLECTED SLAB REACTOR

by

James Hugh McFadden

A Dissertation Submitted to the
Graduate Faculty in Partial Fulfillment of
The Requirements for the Degree of
DOCTOR OF PHILOSOPHY

Major Subject: Nuclear Engineering

Approved:

Signature was redacted for privacy.
In Charge of Major Work

Signature was redacted for privacy.
Head of Major Department

Signature was redacted for privacy.
Dean of Graduate College

Iowa State University
Ames, Iowa

1968

TABLE OF CONTENTS

I. INTRODUCTION

The solution of the space and time dependent neutron kinetics equations poses one of the most important problems in reactor kinetics. Due to the trend toward large thermal reactors, the neutronics of the system can no longer be adequately described by the space independent point reactor kinetics formulation (1,2,3). The point reactor kinetics method calculates an average neutron density distribution whose shape does not change with time. It is obvious that an approach of this type cannot describe any local changes in the flux shape which, for example, might result from the large movement of a single control rod.

The first effort towards a space and time dependent formulation was made by Henry (4). Starting with the transport equation, Henry cast the neutron equations in a form similar to that of the point reactor kinetics. The neutron density $N(r,t)$ is represented as a time dependent shape function $n(r,t)$ multiplied by a time coefficient $T(t)$. The nuclear parameters such as reactivity and lifetime are also functions of space and time through $n(r,t)$. A difficulty arises when this formulation is used to solve a particular problem. In general, an approximation must be made and the common one is to represent $n(r,t)$ by the steady state distribution $n_o(r)$. This is an approximation

which will yield valid solutions only in specific problems.

In an attempt to overcome this difficulty, several other methods were developed to solve the neutron kinetics problem. Henry and Curlee (5) extended the method discussed previously by representing the shape function at a given time by the fundamental mode corresponding to the reactor conditions at that time. The limitation of this method, known as the adiabatic approximation, lies in the fact that a shape function must be calculated at different times, the number of which may prove to be great when considering large transients.

Another method of studying the space-time problem is nodal analysis and has been applied to the reactor kinetics problem by Avery (6). The scheme of this method is to divide the reactor into regions and calculate volume averaged fluxes for each region. These quantities are functions only of time, and the resulting equations are similar to the point reactor kinetics equations. The spatial dependence of the problem is introduced by leakage terms from one region to another. For N nodes, there are 2N coupled first order differential equations which must be solved.

A third method used to determine approximate solutions to the space-time reactor kinetics problem is known as modal analysis. In this method the neutron flux is approximated

by a finite sum of space modes multiplied by time coefficients. The space modes are known functions and the solution to the problem then lies in a determination of the time coefficients. Based on the type of space functions employed, this method may be divided into two types.

In the first type, the space modes are members of an orthogonal set of functions. Foderaro and Garabedian (7) used Helmholtz modes to study the time response of a coupled core reactor, and Loewe (8) investigated the space-dependent frequency response of a reflected slab reactor with these modes as the space functions. The most serious defect of these modes is that a great number are necessary to describe the flux shape in a reactor with even the slightest geometrical complication.

The natural modes (9,10), which are the eigenfunctions associated with the eigenvalues of the steady state matrix operator, also form an orthogonal set. These modes are well suited to the solution of the neutron diffusion equation as they possess the property of finality (9). These functions are substituted into the differential equation and multiplied by an orthogonal weighting function (adjoint modes). Integration over the reactor volume yields a set of N linear first order differential equations for the N time coefficients.

Two other sets of orthogonal space functions are the omega modes (9) and the lambda modes (11). These functions

are also the eigenfunctions of an eigenvalue problem, however when they are substituted into the differential equation, multiplied by an orthogonal weighting function, and integrated over space, a set of coupled first order differential equations results. The solution employing either of these sets of modes is thus harder to obtain due to the difficulty in finding the time coefficients.

The second type of space modes employed in modal expansions are non-orthogonal. The utility of these functions lies in the fact that their selection can be based on some a priori knowledge the investigator has of the perturbation to be studied. The first application of non-orthogonal space modes was made by Dougherty and Shen (12) who used Green's function modes. A modified version of these modes was employed by Carter and Danofsky (13,14) to study time dependent problems, and by Merritt (15) to study the space dependent frequency response of a coupled-core reactor. Yasinsky (16) also has studied the time problem using a version of the Green's function modes.

Another use of non-orthogonal modes has been found in the synthesis technique, applied first to the steady state problem, and then to time dependent problems (17, 18). The synthesis technique was recently extended to two space dimensions and time (19).

The time varying coefficients accompanying the non-orthogonal modes are found by some variational method,

most commonly by the Kantorovich variational method (20). Many variational principles have been proposed for the neutron kinetics problem, but they all can be classed as a version of the image system introduced by Morse and Feshbach (21). Because the diffusion problem is a dissipative process, the differential equations are non-self adjoint, specifically in the term involving the first time derivative. It is in the sense that a sign reversal occurs on this term while going from the diffusion equations to their adjoint equations that the adjoint equations represent an image system. Lewins (22,23) first used this principle for a time dependent problem in reactor theory, and Pomraning (24) subsequently brought together the different versions of this principle into a general formulation.

Another method of solution of the neutron kinetics equations involves the use of finite difference techniques. The two most common codes employing this technique are WIGLE (25) and WIGLE-40 (26), which solve the two energy group, time dependent diffusion equations in one space dimension, including feedback effects. These codes are considered to yield the "exact" solution of the neutron diffusion equations and are used in the comparison of approximate solutions.

In this dissertation, the space functions to be employed are the Green's function modes. In previous

applications of these modes, the reactor has been divided into regions in which the nuclear parameters are constants. In many problems this approach may lead to the use of more trial functions than are necessary to adequately describe the solution. Two immediate reasons for limiting the number of modes to the fewest number necessary are; (1) the computation time for the complete solution increases by approximately twice the number of modes employed, and (2) with the advent of two dimensional space-time studies, the necessary core storage will increase by approximately N^2 over the one space dimension problem.

In the method to be presented, which will be termed the coupled mode approach, the reactor may be divided into regions which contain non-constant nuclear parameters. These regions are made up of subregions within which the nuclear parameters are constant. A reflected slab reactor will be the model in this investigation, and will be subjected to step changes in the thermal absorption cross-section in different regions. The results are to be compared with the exact solutions determined by WIGLE-40 and with approximate solutions determined by the trial functions as proposed by Carter (14). The frequency response of the reactor also will be determined for various sets of trial functions.

II. MATHEMATICAL ANALYSIS WITH THE GREEN'S FUNCTION MODES

A. Reactor Model

The reactor model for this investigation is a reflected reactor and is the same system as was used by Loewe (8). The width of the fuel region is 37 cm and the semi-infinite slab reflectors have a width of 15 cm. The model is representative of an enriched uranium, light water moderated and reflected reactor.

The first step in the application of the Green's function modes to the reactor problem is to determine the steady state flux and the steady state adjoint flux distributions. These

Table II.1. Steady state nuclear parameters

Parameter	Units	Core	Reflector
v_f^{-1}	sec/cm	$3.50(10^{-7})$	$3.50(10^{-7})$
v_s^{-1}	sec/cm	$4.55(10^{-6})$	$4.55(10^{-6})$
D_f	cm	1.24	1.14
D_s	cm	0.26	0.16
Σ_{r1}	cm^{-1}	0.0207	0.0346
p	----	1.0	1.0
Σ_{a1}	cm^{-1}	0.0	0.0
Σ_{r2}	cm^{-1}	0.0816895	0.0118
$\upsilon\Sigma_f$	$\frac{\text{neutrons}}{\text{fission-cm}}$	0.0985	0.0

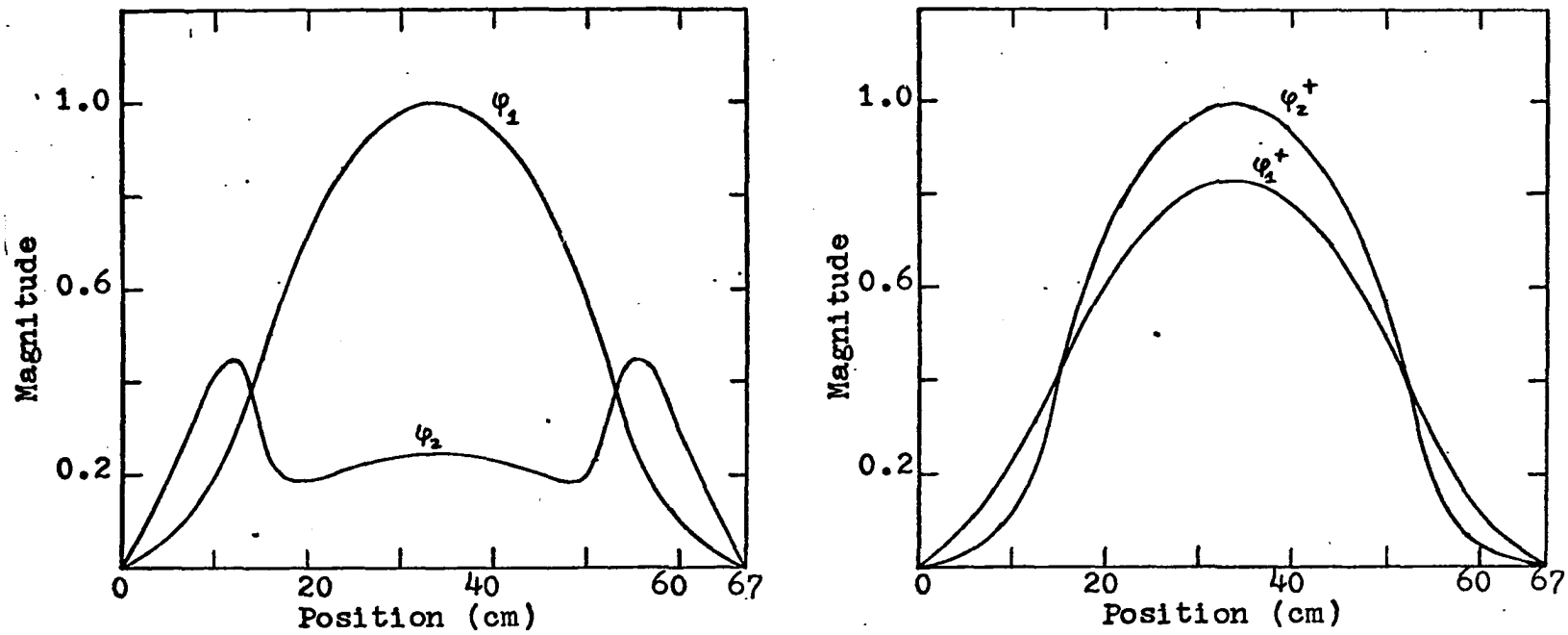

Figure II.1. Critical flux and adjoint flux distributions

were determined by solving the homogeneous set of equations describing the continuity of flux and the continuity of current at steady state. The determinant of the coefficients is zero for a non-trivial solution. To obtain this condition the removal cross-section for the thermal group in the fuel region was varied, and a critical value of $\Sigma_{r2} = 0.0816895$ cm^{-1} was obtained. This value differed only slightly from the value reported by Loewe, $\Sigma_{r2} = 0.0818$ cm^{-1}. The steady state nuclear parameters are given in Table II.1. The constants in the equations for the flux and the adjoint flux were determined with the routine GINV2 which is designed to solve a set of homogeneous algebraic equations.

The steady state flux and adjoint flux distributions are shown in Figure II.1, with the fast group flux and the thermal group adjoint flux normalized to unity at the center of the reactor.

B. Modifications in the Formulation of the Space Functions

In this section the method proposed to determine the space functions will be presented. The neutron diffusion equations, neglecting delayed neutrons and external sources, are given in Appendix A as

$$\vec{\nabla} \cdot D \vec{\nabla} \varphi + H\varphi + Q\varphi = V^{-1} \frac{\partial}{\partial t} \varphi \quad . \quad \text{(II.1)}$$

For the two group neutron diffusion equation, subject to the condition that all fissions occur in the thermal group and all fission neutrons enter the fast group, the matrices in

Eq. II.1 are given by

$$D = \begin{bmatrix} D_1 & 0 \\ 0 & D_2 \end{bmatrix} \qquad H = \begin{bmatrix} -\Sigma_{r1} & 0 \\ \Sigma_{r1} & -\Sigma_{r2} \end{bmatrix} \qquad \varphi = \begin{bmatrix} \varphi_1 \\ \varphi_2 \end{bmatrix}$$

$$Q = \begin{bmatrix} 0 & \nu\Sigma_f \\ 0 & 0 \end{bmatrix} \qquad V^{-1} = \begin{bmatrix} 1/v_1 & 0 \\ 0 & 1/v_2 \end{bmatrix}$$

The elements of D, H, V^{-1} and Q are region-wise constants.

The method employed for the solution of Eq. II.1 by a modal analysis technique is to represent the solution by a finite sum of known space functions multiplied by the corresponding time coefficients

$$\varphi(r,t) = \sum_{i=1}^{N} a_i(t)\, \psi_i(r) \qquad . \qquad \text{(II.2)}$$

The basic approach to the determination of the space functions is discussed in Appendix B. The discussion which follows will focus on the proposed modifications to the construction of these modes. Two types of modal coupling will be considered. The first type is the coupling of an entire non-multiplying region to a fuel region and the second type is the coupling of a portion of a non-multiplying region to a fuel region.

As an example of the construction of space modes of the first type, the reactor is divided into four regions as shown in Figure II.2. The first region includes the left reflector (subregion a) and part of the fuel region (subregion b). The second and third regions are completely in the fuel, and the fourth region is in the right reflector. The Green's function approach calls for distributed sources to be placed in each of

these regions, as discussed in Appendix B. The boundary conditions on the space functions apply as do the continuity conditions for the mode and the modal current at each interior surface. The condition that the modes sum to the steady state flux and steady state adjoint flux distribution also must be fulfilled.

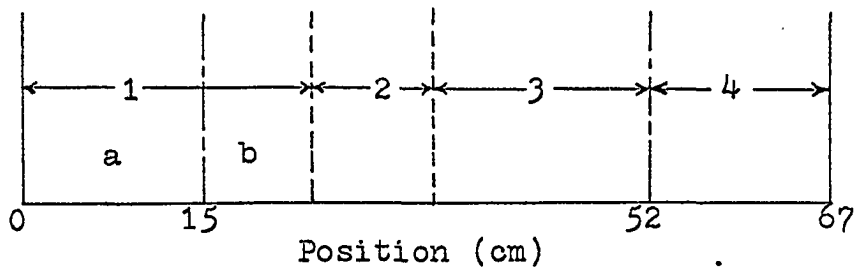

Figure II.2. Division of reactor for sample problem

The construction of the modes with the source terms in regions two, three, and four is the same as described in Appendix B. In the first region a different scheme is used. The equations for the first mode in the fast group in Table B.1 in Appendix B indicate that this mode is negative. The same is true of the first adjoint mode for the thermal group. In this coupled mode method, these two modes are treated without any source term in the reflector subregion and with the fuel source term in the fuel subregion. Thus the equations for the fast group modes in region one are given by

$$\vec{\nabla} \cdot D_1 \vec{\nabla} \psi_i - \Sigma_{r1o} \psi_i = 0 \qquad i = 1, \ldots, 4 \qquad \text{(II.3)}$$

for subregion a and

$$\vec{\nabla} \cdot D_2 \vec{\nabla} \psi_i - \Sigma_{r2o} \psi_i = \begin{cases} -\nu \Sigma_f \varphi_{2o} & i = 1 \\ 0 & i \neq 1 \end{cases} \qquad \text{(II.4)}$$

for subregion b. The equations for the thermal group adjoint modes in region one are given by

$$\vec{\nabla} \cdot D_2 \vec{\nabla} \psi_i^+ - \Sigma_{r2o} \psi_i^+ = 0 \qquad i = 1, \cdots, 4 \qquad \text{(II.5)}$$

for subregion a and by

$$\vec{\nabla} \cdot D_2 \vec{\nabla} \psi_i^+ - \Sigma_{r2o} \psi_i^+ = \begin{cases} -\nu\Sigma_f \varphi_{1o}^+ & i = 1 \\ 0 & i \neq 1 \end{cases} \qquad \text{(II.6)}$$

for subregion b. The first mode for the second group and the first adjoint mode for the first group are treated as in Appendix B, that is, with a source term for each mode in the two subregions. The modes for the two subregions are coupled at the interface with the continuity conditions.

To illustrate the second type of modal coupling, the reactor is divided into four regions as shown in Figure II.3. The first region is in the left reflector. The second region

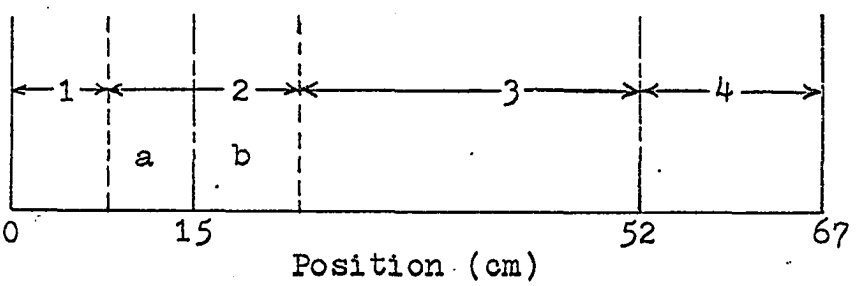

Figure II.3. Division of reactor for sample problem

is partially in the left reflector (subregion a) and partially in the fuel (subregion b). The third region is in the fuel and the fourth region is in the right reflector.

The construction of the modes with the source terms in regions three and four is the same as described in Appendix B. If the removal cross-sections in region one and subregion a

of region two are divided as indicated in Eq. B.11, the second mode for the fast group and the modal current are discontinuous at the interface between the first and second regions. The same is true for the second adjoint mode for the thermal group. Thus the removal cross-sections in the left reflector are divided as given by

$$\Sigma_{ri_0} = \Sigma_{ri}' - \Sigma_{ri}'' \quad . \qquad \text{(II.7)}$$

It is to be noted that Σ_{ri}' is larger than Σ_{ri_0}, thus the modes with the source term in the left reflector are now positive and the mode and the modal current are continuous at the region interfaces.

With the redistribution of the removal cross-sections as given by Eq. II.7, the two modes are treated with a source term in each region. The equations for the fast group modes in region one are

$$\vec{\nabla} \cdot D_1 \vec{\nabla} \psi_i - \Sigma_{r1}' \psi_i = \begin{cases} -\Sigma_{r1}'' \varphi_{10} & i = 1 \\ 0 & i \neq 1 \end{cases} \qquad \text{(II.8)}$$

and the equations for the thermal group adjoint modes in region one are given by

$$\vec{\nabla} \cdot D_2 \vec{\nabla} \psi_i^+ - \Sigma_{r2}' \psi_i^+ = \begin{cases} -\Sigma_{r2}'' \varphi_{20}^+ & i = 1 \\ 0 & i \neq 1 \end{cases} \quad . \qquad \text{(II.9)}$$

The equations for the fast group modes in region two are

$$\vec{\nabla} \cdot D_2 \vec{\nabla} \psi_i - \Sigma_{r1}' \psi_i = \begin{cases} -\Sigma_{r1}'' \varphi_{10} & i = 2 \\ 0 & i \neq 2 \end{cases} \qquad \text{(II.10)}$$

for subregion a and

$$\vec{\nabla}\cdot D_1 \nabla\vec{\psi}_i - \Sigma_{r1o}\psi_i = \begin{cases} -\nu\Sigma_f \varphi_{2o} & i=2 \\ 0 & i\neq 2 \end{cases} \qquad \text{(II.11)}$$

for subregion b. The equations for the thermal group adjoint modes in region two are

$$\nabla\cdot D_2 \nabla\psi_i^+ - \Sigma_{r2}'\psi_i^+ = \begin{cases} -\Sigma_{r2}''\varphi_{2o}^+ & i=2 \\ 0 & i\neq 2 \end{cases} \qquad \text{(II.12)}$$

for subregion a and

$$\nabla\cdot D_2 \nabla\psi_i^+ - \Sigma_{r2o}\psi_i^+ = \begin{cases} -\nu\Sigma_f \varphi_{2o}^+ & i=2 \\ 0 & i\neq 2 \end{cases} \qquad \text{(II.13)}$$

for subregion b.

The procedure to determine the space modes and the adjoint space modes may be summarized as;

1. Calculate the steady state flux and adjoint flux distributions.
2. Divide the reactor into N regions.
3. The space mode and the adjoint space mode for the ith region are calculated by substituting the source term into the ith region and zero source elsewhere. Eq. B.9 and Eq. B.10 are used to calculate the modes.
4. The source terms are found in the following way;
   a. if the nuclear parameters are constant across each region the source terms are found as indicated in Appendix B.
   b. if the nuclear parameters are constant only for subregions, the sources are found as discussed in the preceeding pages.

C. The Variational Principle for Time Dependent Problems

The variational principle for the neutron diffusion problem is given in Appendix A by Eq. A.10. The Kantorovich method (20) of solution involves the use of known space trial functions with unknown time dependent coefficients. The solution of the time coefficients is such as to render the variational principle stationary.

From the set of admissible trial functions for the functional, a subset is chosen of the form

$$u(r,t) = \sum_{i=1}^{N} \psi_i(r)\, a_i(t) = \Psi \underline{a} \qquad \text{(II.14)}$$

where $$\Psi = \text{diag}\left[\psi_1^1, \cdots, \psi_1^N, \psi_2^1, \cdots, \psi_2^N\right] \qquad \text{(II.15)}$$

and $$\underline{a} = \left[a_1^1, \cdots, a_1^N, a_2^1, \cdots, a_2^N\right]^T \quad . \qquad \text{(II.16)}$$

The subset of admissible adjoint trial functions is chosen as

$$u^+(r,t) = \sum_{i=1}^{N} b_i(t)\, \psi_i^+(r) = \underline{b}\Psi^+ \qquad \text{(II.17)}$$

where $$\Psi^+ = \text{diag}\left[\psi_1^{1+}, \cdots, \psi_1^{N+}, \psi_2^{1+}, \cdots, \psi_2^{N+}\right] \qquad \text{(II.18)}$$

and $$\underline{b} = \left[b_1^1, \cdots, b_1^N, b_2^1, \cdots, b_2^N\right] \quad . \qquad \text{(II.19)}$$

The Kantorovich method of solution is to substitute the trial functions into the variational principle and perform the space integrations before taking the variations in the time coefficients. Substitution of the trial functions into the variational principle yields

$$L[\varphi^+,\varphi] = \int_{t_0}^{t_2} dt \int_V dr \left\{ \sum_{i,j=1}^{N} \left[\frac{1}{2}\left(b_j \psi_j^+ V^{-1} \psi_i \frac{da_i}{dt} - \frac{db_j}{dt} \psi_j^+ V^{-1} \psi_i a_i \right) \right.\right.$$

$$\left.\left. + b_j \vec{\nabla}\psi_j^+ \cdot D \vec{\nabla}\psi_i a_i - b_j \psi_j^+ (K+Q)\psi_i a_i \right]\right\} + \int_{t_0}^{t_1} dt \oint_{\Gamma_a} dS_a \sum_{i,j=1}^{N} b_j \psi_j^+ \psi_i a_i$$

$$- \frac{1}{2} \int_V dr \sum_{i,j=1}^{N} \left\{ \left[b_j \psi_j^+ V^{-1} \psi_i a_i \right]\Big|_{t_1} + \left[b_j \psi_j^+ V^{-1} \psi_i a_i \right]\Big|_{t_0} \right\} . \qquad \text{(II.20)}$$

With the space integrations defined by

$$\int_V dr\, \psi_j^+ P \psi_i = P_{ji} \qquad \text{(II.21)}$$

the variational principle can be written as

$$L[\varphi^+,\varphi] = \int_{t_0}^{t_2} dt \left\{ \sum_{i,j=1}^{N} \left[b_j \left(\frac{1}{2} V_{ji} \frac{da_i}{dt} + (D_{ji} - K_{ji} - Q_{ji}) a_i \right) - \frac{1}{2} \frac{db_j}{dt} V_{ji}^{-1} a_i \right] \right\}$$

$$+ \int_{t_0}^{t_2} dt \oint_{\Gamma_a} dS_a \sum_{i,j=1}^{N} b_j \psi_j^+ \psi_i a_i - \frac{1}{2} \sum_{i,j=1}^{N} \left\{ \left[b_j V_{ji} a_i \right]\Big|_{t_1} + \left[b_j V_{ji} a_i \right]\Big|_{t_0} \right\} . \qquad \text{(II.22)}$$

It is shown in Appendix A that a variation in the adjoint flux leads to the Euler-Lagrange equation for the flux. The same procedure used in Appendix A for the variation $\delta\varphi^+$ is now used for the variation δb_j with the result

$$\delta L_1[\varphi^+,\varphi] = 0 = \int_{t_0}^{t_1} dt \left\{ \sum_{i,j=1}^{N} \delta b_j \left[V_{ji} \frac{da_i}{dt} + (D_{ji} - K_{ji} - Q_{ji}) a_i \right] \right\}$$

$$- \sum_{i,j=1}^{N} \left[\delta b_j V_{ji} a_i \right]\Big|_{t_1} . \qquad \text{(II.23)}$$

Since the δb_j are arbitrary and independent, and because $\delta b_j(t_1) = 0$, the result is a system of N first order

differential equations for the $a_i(t)$

$$\sum_{i=1}^{N} \left[V_{ji} \frac{da_i}{dt} + \left(D_{ji} - K_{ji} - Q_{ji} \right) a_i \right] = 0 \qquad j = 1, 2, \cdots, N. \tag{II.24}$$

Equation II.24 can be written as

$$\Lambda \frac{d}{dt} \underline{a} = K \underline{a} \tag{II.25}$$

where

$$\Lambda = \begin{bmatrix} V_{1,1} & \cdots & V_{1,2N} \\ \vdots & & \\ V_{2N,1} & & V_{2N,2N} \end{bmatrix} \qquad K = \begin{bmatrix} (D-K-Q)_{1,1} & \cdots & (D-K-Q)_{1,2N} \\ \vdots & & \\ (D-K-Q)_{2N,1} & & (D-K-Q)_{2N,2N} \end{bmatrix}$$

Two methods of solving Eq. II.25 are considered. The first method is a numerical integration scheme which utilizes the Runge-Kutta technique (27). The routine which is to be used in the solution is the routine NODE, as written in Fortran for the IBM 360/65 computer.

The second method is applicable if the coefficients of Λ and K are constant in time. This is the case for a step change in a nuclear parameter at time $t = t_o^+$. Solutions to Eq. II.25 of the form $a_i^j(t) = \alpha_i^j e^{\omega t}$ are assumed which lead to an eigenvalue problem for ω,

$$\omega \Lambda \underline{\alpha} = K \underline{\alpha} \tag{II.26}$$

where $$\alpha = \left[\alpha_1^1, \cdots, \alpha_1^N, \alpha_2^1, \cdots \alpha_2^N \right]^T \tag{II.27}$$

Since Λ is a non-singular matrix, an inverse exists and Eq. II.26 may be written as

$$\Lambda^{-1} K \underline{\alpha} = \omega \underline{\alpha} \tag{II.28}$$

If no degeneracy exists the solution of Eq. II.28 will yield 2N eigenvalues, ω_ν , and 2N eigenvectors, α_ν. The time coefficient $a_i^j(t)$ is given by

$$a_i^j(t) = \sum_{\nu=1}^{2N} \alpha_i^{j\nu} e^{\omega_\nu t} \quad . \qquad \text{(II.29)}$$

The solution for the fast group flux is

$$\varphi_1(r,t) = \sum_{j=1}^{N} \sum_{\nu=1}^{2N} \alpha_1^{j\nu} e^{\omega_\nu t} \psi_1^j(r) \qquad \text{(II.30)}$$

and the solution for the thermal group flux is

$$\varphi_2(r,t) = \sum_{j=N+1}^{2N} \sum_{\nu=1}^{2N} \alpha_2^{j\nu} e^{\omega_\nu t} \psi_2^j(r) \quad . \qquad \text{(II.31)}$$

The eigenvectors α_i^j are normalized such that the solutions given by Eq. II.30 and Eq. II.31 sum to the initial steady state fluxes for the respective energy groups. These normalization conditions are

$$\sum_{\nu=1}^{2N} \alpha_1^{i\nu} = 1 \qquad i = 1, 2, \cdots, N$$

$$\sum_{\nu=1}^{2N} \alpha_2^{i\nu} = 1 \qquad i = N+1, N+2, \cdots, 2N \quad . \qquad \text{(II.32)}$$

D. The Variational Principle for Frequency Dependent Problems

To determine the frequency response of the reactor to a localized oscillator at $r = r_0$, the thermal group removal cross-section is varied sinusoidally about the steady state

value, Σ_{r2o} , according to

$$\Sigma_{r2}(r,t) = \Sigma_{r2o} + \delta\Sigma_{r2} e^{j\omega t} \delta(r-r_o) \qquad \text{(II.33)}$$

where $\delta\Sigma_{r2}$ is the amplitude of the oscillation, and $\delta\Sigma_{r2} << \Sigma_{r2o}$.

When Eq. II.33 is substituted into the variational principle given by Eq. II.20, integrating over the reactor volume and performing the variation δb_j^+ yields an equation for the $a_i(t)$ of the form

$$\Lambda \frac{d}{dt} \underline{a} = \left(K_o + \delta K \right) \underline{a} \qquad \text{(II.34)}$$

where the elements of K_o are dependent only on the steady state nuclear parameters. The elements of δK are given by

$$\left[\delta K\right]_{ji} = \langle \psi_j^+ \left| \delta\Sigma_{r2} \delta(r-r_o) \right| \psi_i \rangle \quad .$$

The flux is assumed to oscillate about the steady state distribution with the same frequency as the oscillator but with different magnitude and phase. Thus the time coefficients may be written as

$$\underline{a} = \underline{a_o} + \underline{\delta a}\, e^{j\omega t} \qquad \text{(II.35)}$$

where $\underline{a_o} = \left[1, 1, \cdots, 1\right]^T$

and $\underline{\delta a} = \left[\delta a_1^1, \ldots, \delta a_1^N, \delta a_2^1, \ldots, \delta a_2^N\right]^T$.

Equation II.35 is substituted into Eq. II.34, yielding

$$j\omega\, e^{j\omega t}(\Lambda \underline{\delta a}) = K_o \underline{a_o} + \delta K \underline{a_o} + e^{j\omega t}(K_o \underline{\delta a} + \delta K \underline{\delta a})$$

$$= \delta K \underline{a_o} + e^{j\omega t}(K_o \underline{\delta a}) \quad . \qquad \text{(II.36)}$$

To arrive at the final form of Eq. II.36, the second order

term $\delta K \delta a$ was neglected and the term $K_o a_o$ was recognized as the critical condition.

It is noted that the coefficients for the space functions are complex numbers which may be written as

$$\delta a_i^k = \mu_i^k + j \nu_i^k \quad . \quad \text{(II.37)}$$

Equation II.36 can now be written as

$$\left[j\omega \Lambda - K_o \right] \begin{bmatrix} \mu_1^1 + j\nu_1^1 \\ \vdots \\ \mu_2^N + j\nu_2^N \end{bmatrix} = \left[\left\langle \psi_k^+ \left(\delta \Sigma_{r2} \delta(r - r_o) \right) \psi_i \right\rangle \right] \begin{bmatrix} 1 \\ \vdots \\ 1 \end{bmatrix} . \quad \text{(II.38)}$$

The μ_i and ν_i are found by separating Eq. II.38 into 2N equations representing the real part of Eq. II.38 and 2N equations representing the imaginary part.

The expression for the flux is

$$\varphi(r,\omega) = \sum_{i=1}^{N} \psi_i(r)\, a_i(\omega)$$

$$= \sum_{i=1}^{N} \psi_i(r) \mu_i(\omega) + j \sum_{i=1}^{N} \psi_i(r) \nu_i(\omega)$$

or $$\varphi(r,\omega) = R(r,\omega) + j\, \Im(r,\omega) \quad . \quad \text{(II.39)}$$

The magnitude and the phase of the frequency are given by

$$\text{magnitude} = \left[R^2 + \Im^2 \right]^{1/2} \quad \text{(II.40)}$$

$$\text{phase} = \tan^{-1} \Im / R \quad . \quad \text{(II.41)}$$

III. APPLICATION TO TIME DEPENDENT PROBLEMS

A. Problem One

In this section the time response of the reactor to two perturbations will be investigated for various sets of trial functions. The approximate solutions will be compared with the "exact" solution as calculated by the code WIGLE. Both perturbations are step changes in the second group removal cross-section, and are introduced at time $t = t_o^+$.

The first problem studied was the time response of the system to a step change in the thermal group removal cross-section in the region $15 \leq x \leq 24$ (Figure III.1). This perturbation resulted in a reactivity insertion of 7.45% $\delta k/k$. The exact solution was obtained by WIGLE with a time step of 5.0×10^{-6} sec.

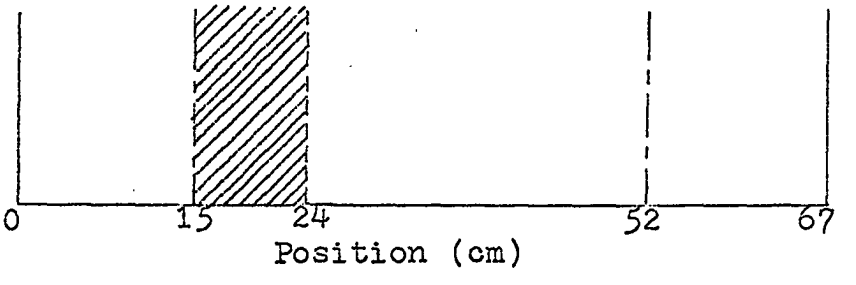

Figure III.1. Division of reactor for problem one

Four sets of trial functions were employed to obtain approximate solutions to Eq. II.1 for this perturbation. The source terms for the first set of trial functions were associated with regions of constant nuclear parameters, as discussed in Appendix B. There were three regions in the fuel

region, including one in the region where the perturbation was introduced, and one region in each reflector, as indicated in Figure III.2.

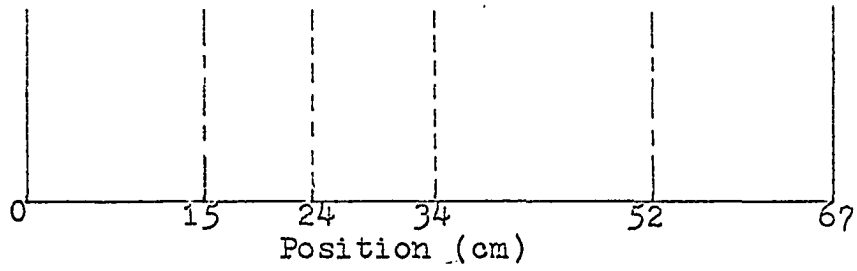

Figure III.2. Division of reactor for 5-M analysis

The negative modes were formed by dividing the removal cross-sections in the reflector regions according to

$$\Sigma_{r1o} = \Sigma_{r1}' + \Sigma_{r1}'' \qquad \text{where } \Sigma_{r1}' = 0.00115 \text{ cm}^{-1}$$

and $$\Sigma_{r2o} = \Sigma_{r2}' + \Sigma_{r2}'' \qquad \text{where } \Sigma_{r2}' = 0.0040 \text{ cm}^{-1}.$$

Carter (14) has shown that the manner in which the removal cross-section is divided does not affect the solution to the problem as long as one of the right hand side terms is non-zero. The space functions and the adjoint space functions for this set of trial functions, denoted by 5-M, are shown in Figures III.3 and III.4.

The flux distributions for the fast group and the thermal group are shown in Figures III.5 and III.6. The asymptotic eigenvalue (reciprocal period) of the exact solution is 2308 sec^{-1} as compared to the asymptotic eigenvalue 2271 sec^{-1} calculated by the eigenvalue problem, Eq. II.28.

The approximate solution and the exact solution agree quite well for the fast flux, especially the transient part of

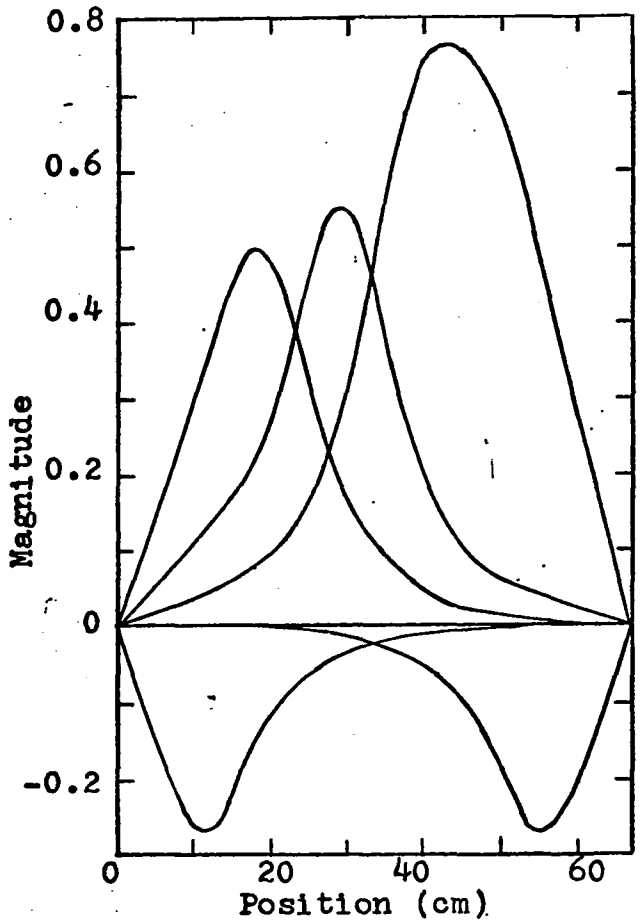

(a) Fast modes

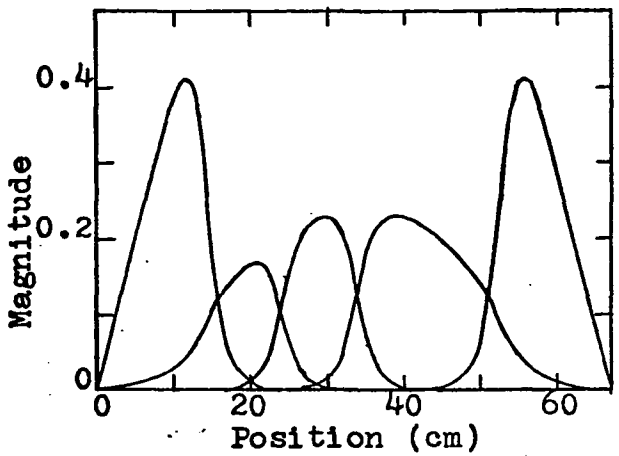

(b) Thermal modes

Figure III.3. Space modes for 5-M analysis

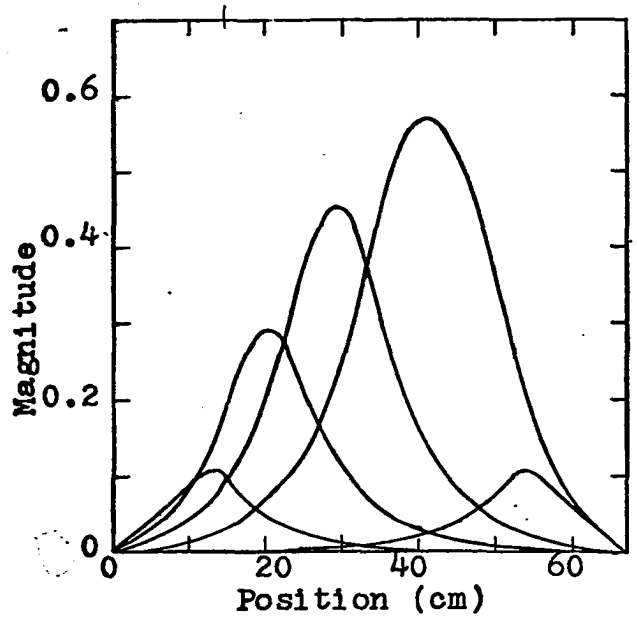

(a) Fast adjoint modes

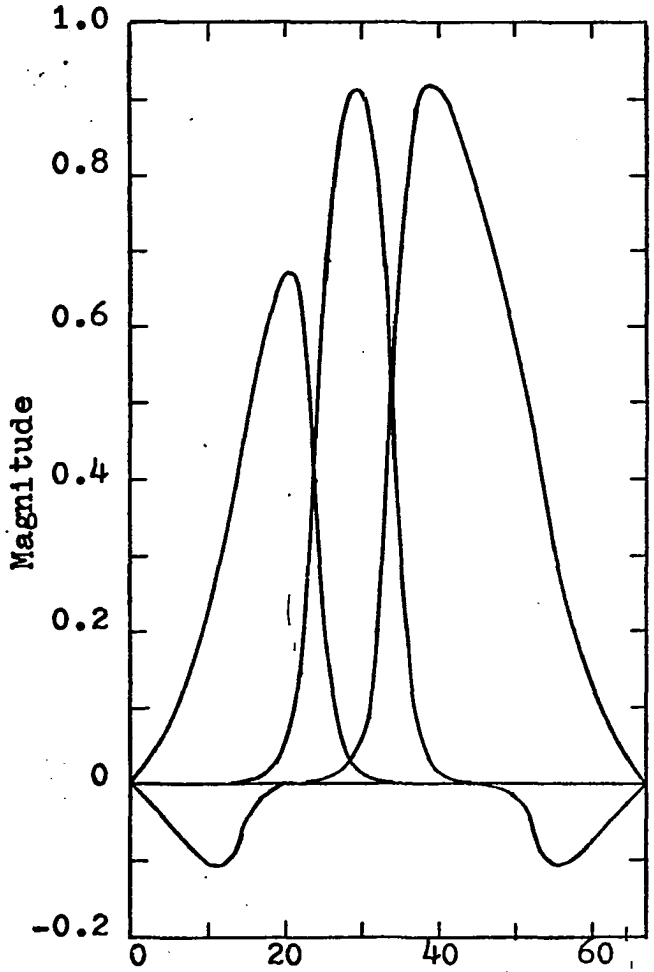

(b) Thermal adjoint modes

Figure III.4. Adjoint space modes for 5-M analy...

the solutions ($t \leq 0.002$ sec). After the transients have decayed and the solution is increasing with a single positive period, the two solutions begin to differ. The differences in the solutions for asymptotic times can be attributed to the different asymptotic eigenvalues for the approximate solution and the exact solution.

The difference between the exact solution and the approximate solution for the thermal flux is more pronounced. The first reason is that the change in the flux shape for the thermal group is much more drastic than for the fast group. The results depicted in Figure III.6 can be discussed by considering three regions. The first region is in the vicinity of the left reflector-fuel interface ($10 \leq x \leq 20$). The change from the initial fuux shape to the final flux shape in this region is almost instantaneous, occurring in less than 0.25 msec. Thus the shape indicated by the approximate solution does not change as time increases, and in fact begins to lag the exact solution as the transients decay.

The shape of the approximate solution in this region does not agree very well with the shape of the exact solution. The reason for this is that the trial functions are based on the steady state flux shape. The flux shape near the interface changes due to the decreased removal of the thermal neutrons in the fuel region and the increased neutron slowing down from the fast group in the reflector region. Thus the part of the distribution which was a minimum at steady state conditions

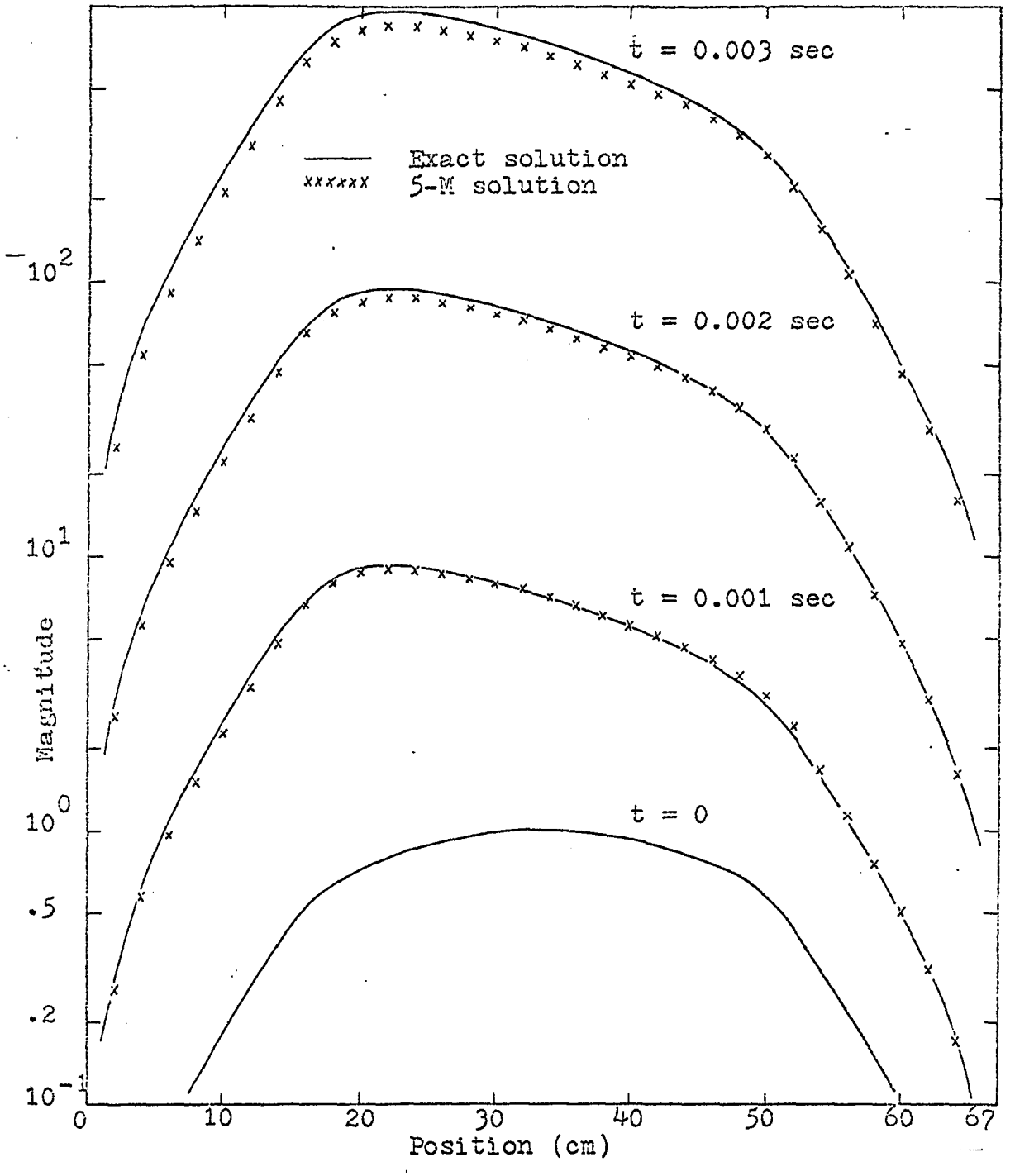

Figure III.5. Fast flux distribution, problem one

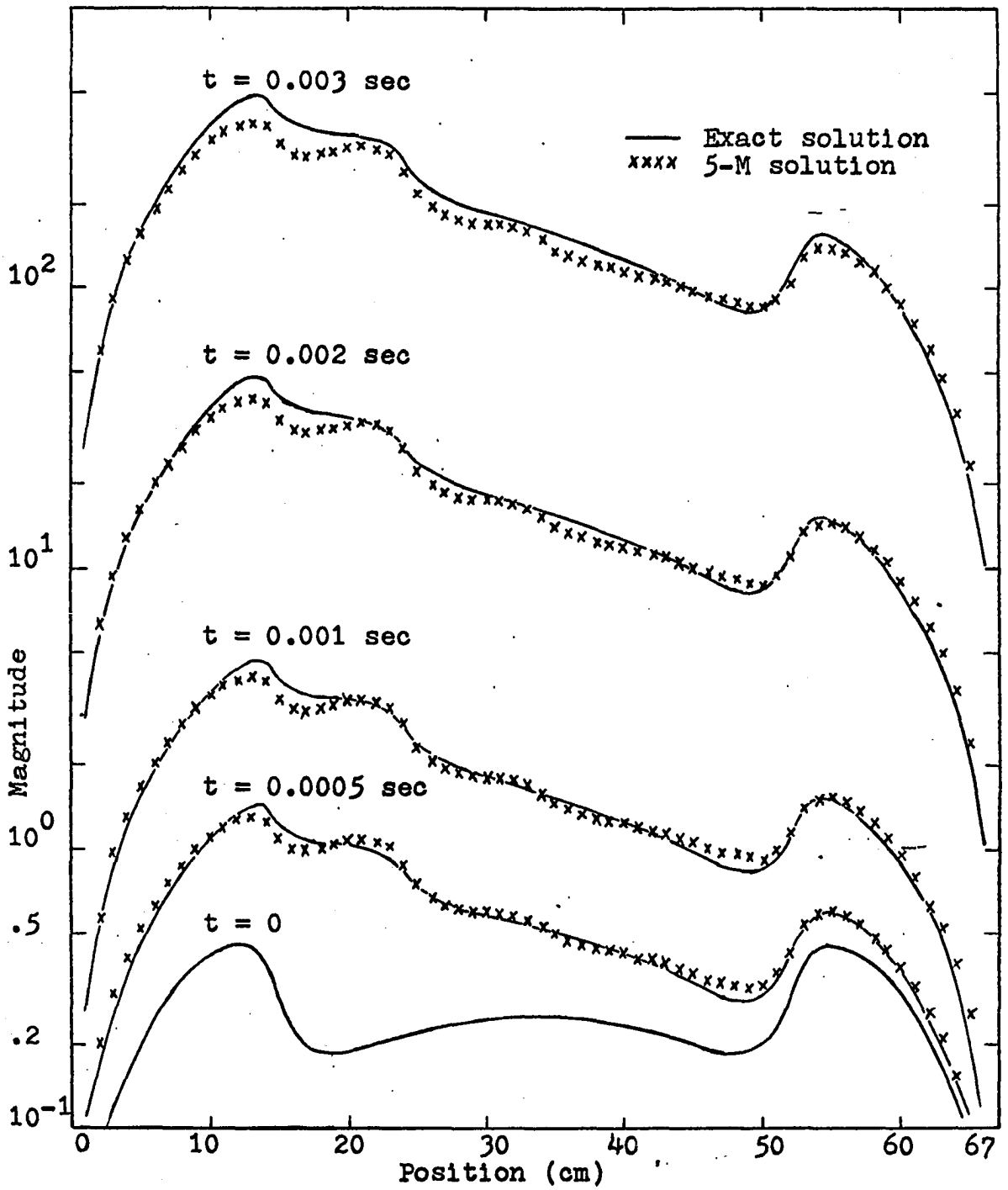

Figure III.6. Thermal flux distribution, problem one

now tends toward a maximum under the perturbed conditions. This event indicates the need for a change in the space modes around this interface.

The second region to be considered is the region in the center of the fuel ($20 \leq x \leq 42$). The approximate and exact solutions in this region agree quite well except for the asymptotic differences. The ripple in the approximate solution is the result of trying to approximate a linear shape with a combination of arcs. This can be accomplished if enough arcs (trial functions) of small arclength are chosen. However for the purposes of this investigation, the results are considered acceptable.

The third region is around the right reflector-fuel interface. The conditions present at the interface on the left side of the reactor are also present in this region, although the change in the flux shape is not as pronounced. The difference in the exact and approximate solutions in the fuel part of this region ($43 \leq x \leq 52$) are due to the fact that this shape is described by one mode. The time coefficient for this mode is in turn influenced more by the rapidly increasing flux in the center of the reactor than it is by the slowly increasing flux in and near the right reflector. A change in the selection of the space functions around this interface also is necessary for a better solution.

There are two methods of improving the solution to this problem. The first is the addition of more space functions.

From the results shown in Figure III.6, this would mean two modes in the left reflector, two modes in the perturbed region, three modes in the unperturbed fuel region, and one mode in the right reflector for a total of eight space functions.

Another solution is to redistribute the present five modes. An indication as to how this might be accomplished may be found by studying the time coefficients for the thermal group space modes, shown in Figure III.7. It is noted that the coefficient for the second mode initially increases much more rapidly than does the coefficient for the first mode. Thus a possible solution to overcome the differences in the exact and approximate solutions near the reflector-fuel interface would be to separate the space function in the perturbed region into two functions. One of these in turn would be coupled to the left reflector mode. This coupling would be expected to result in an initial increase in the slope of the first time coefficient.

At the right reflector interface the modes could be distributed in the same manner. The time coefficient for the fifth mode is initially increasing slower than the coefficient for the fourth mode. Thus the fourth mode could be divided with part of this mode then coupled to the mode in the right reflector.

Based on the conclusions of the foregoing discussion, the reactor was divided into regions as shown in Figure III.8. The source term for the first mode lies in the left reflector

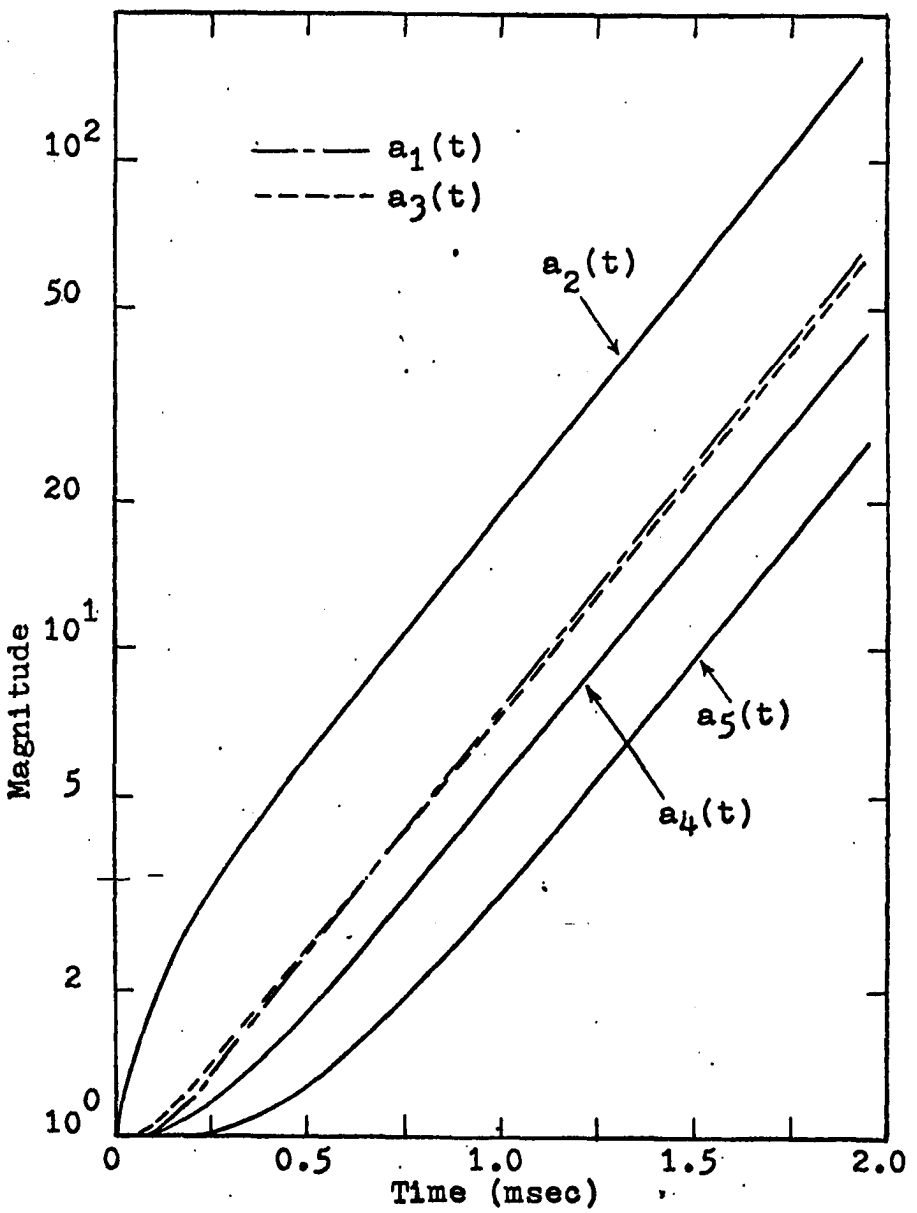

Figure III.7. 5-M thermal mode time coefficients

and part of the perturbed region ($0 \leq x \leq 17$), with the source term for the second mode occupying the remainder of the perturbed region. The third space mode is not changed. The source term for the fourth mode is in the region $34 \leq x \leq 50$, with the source term for the fifth mode occupying the remainder of the fuel region and the right reflector. These space functions and the adjoint space functions are shown in Figures III.9 and III.10. This set of trial functions will be referred to as 5-MC1.

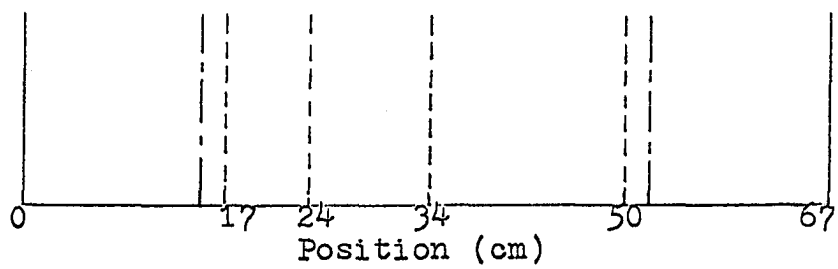

Figure III.8. Division of reactor for 5-MC1 analysis

The flux distributions for the thermal group are shown in Figure III.11. The asymptotic eigenvalue of this approximate solution is 2137 sec^{-1} as compared to the exact eigenvalue of 2308 sec^{-1} and the eigenvalue associated with the 5-M solution of 2271 sec^{-1}. The difference in the asymptotic eigenvalues will be discussed later.

Neglecting the difference in the solutions due to the difference in the asymptotic eigenvalues, Figure III.11 shows that the changes which were made in the selection of the space functions resulted in good agreement between the exact solution and the approximate solution near the right reflector-

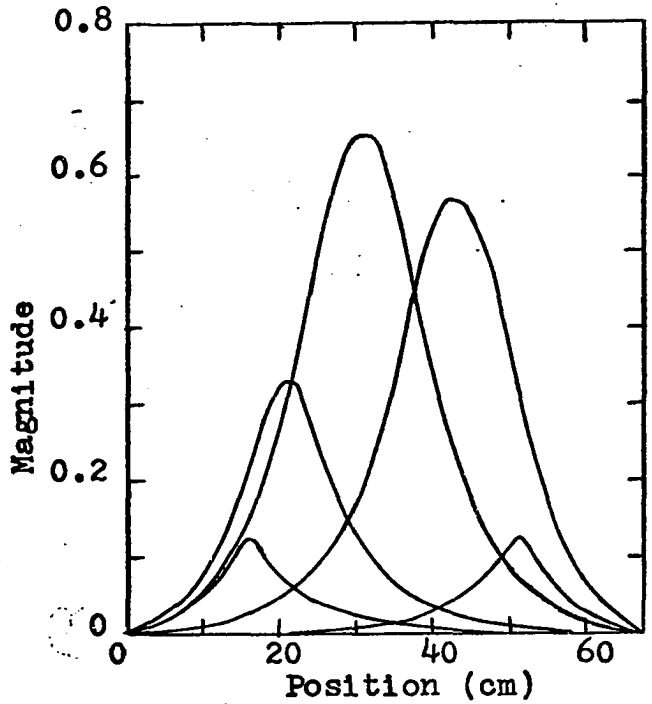

(a) Fast modes

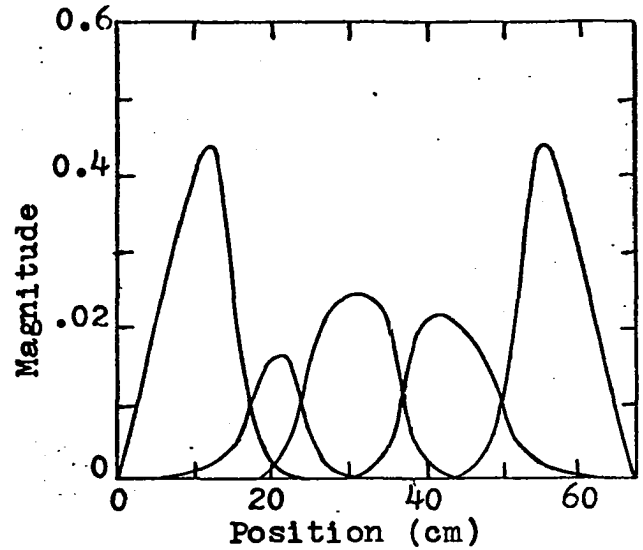

(b) Thermal modes

Figure III.9. Space modes for 5-MC1 analysis

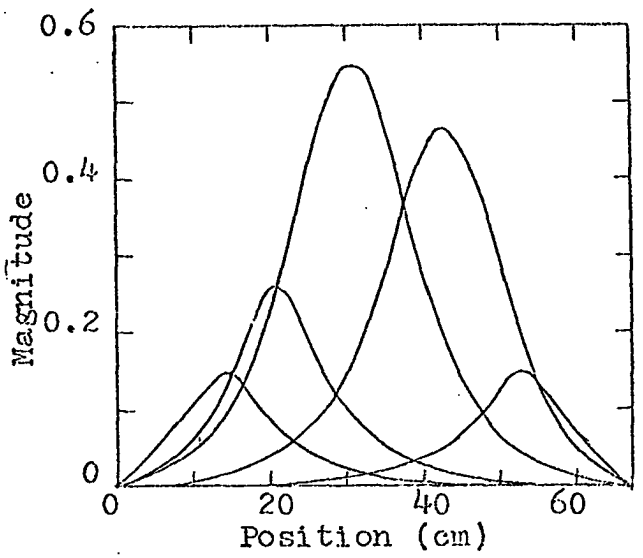

(a) Fast adjoint modes

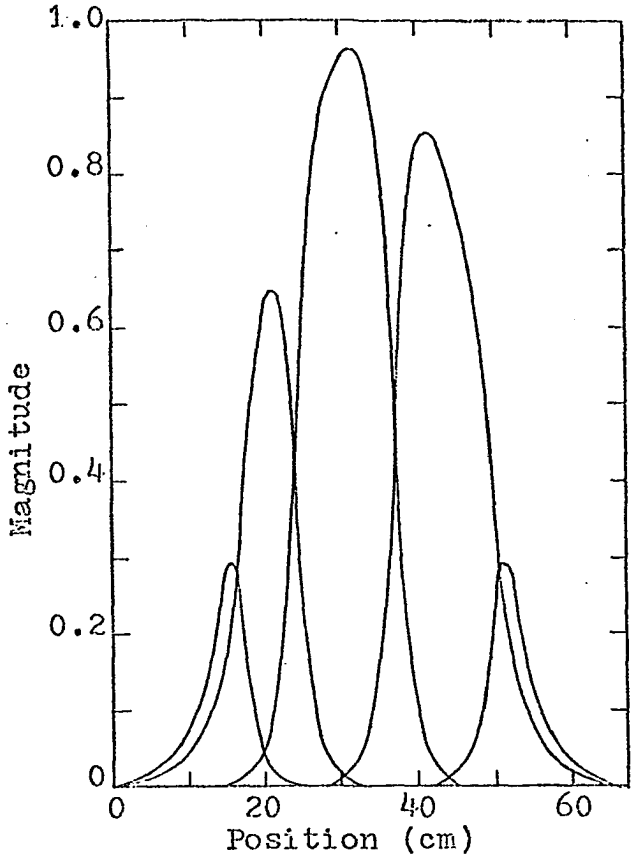

(b) Thermal adjoint modes

Figure III.10. Adjoint space modes for 5-MC1 analysis

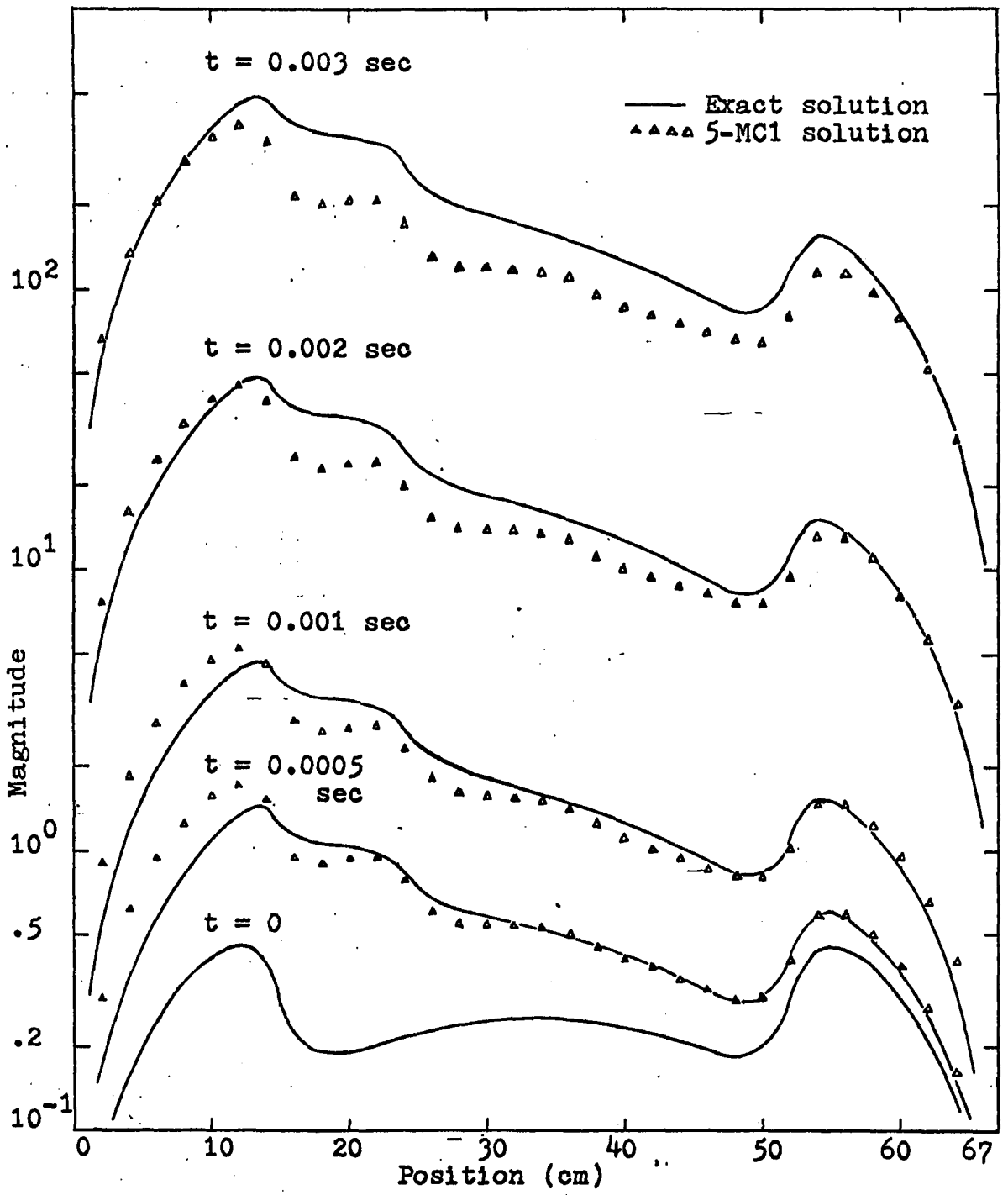

Figure III.11. Thermal flux distribution, problem one

fuel interface. However the solution near the left reflector-fuel interface was not improved. The approximate solution in the reflector shows a higher flux level than does the exact solution. This difference results from coupling too much of the perturbed region to the reflector region.

To improve on the approximate solution near the left reflector-fuel interface, a third set of trial functions was selected with the source terms for the space modes distributed as shown in Figure III.12. The first mode has its source term in the reflector ($0 \leq x \leq 14$). The second mode has its source term in the remaining part of the reflector and in the perturbed region. The third, fourth and fifth modes have the same source terms as in the 5-MC1 set of trial functions. This new set of trial functions will be denoted by 5-MC2.

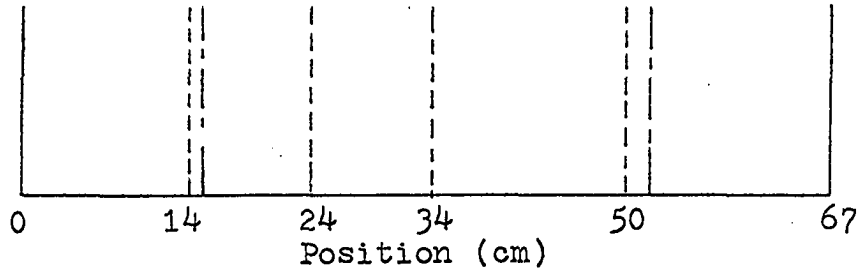

Figure III.12. Division of reactor for 5-MC2 analysis

The removal cross-sections in the left reflector were separated according to Eq. II.7 to keep the second mode for the fast group and the second adjoint mode for the thermal group from being discontinuous in space. In the selection of these modes the removal cross-sections were written as

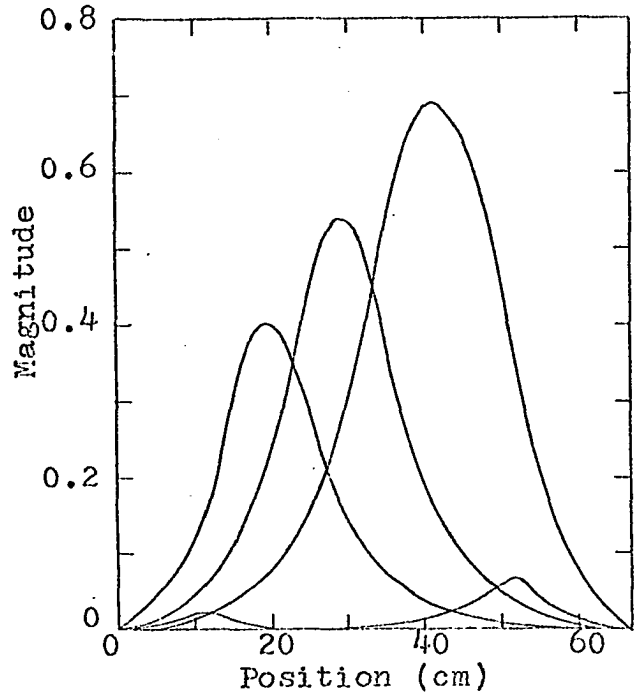

(a) Fast modes

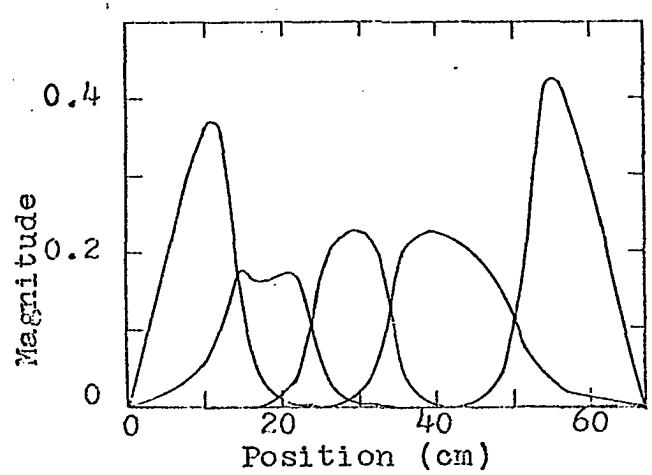

(b) Thermal modes

Figure III.13. Space modes for 5-MC2 analysis

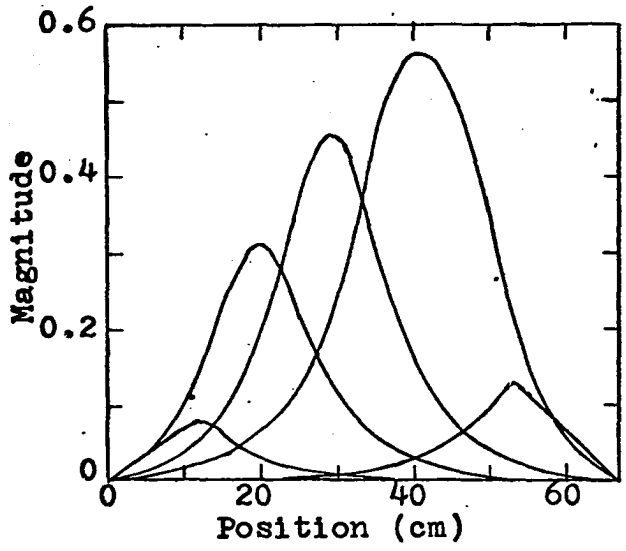

(a) Fast adjoint modes

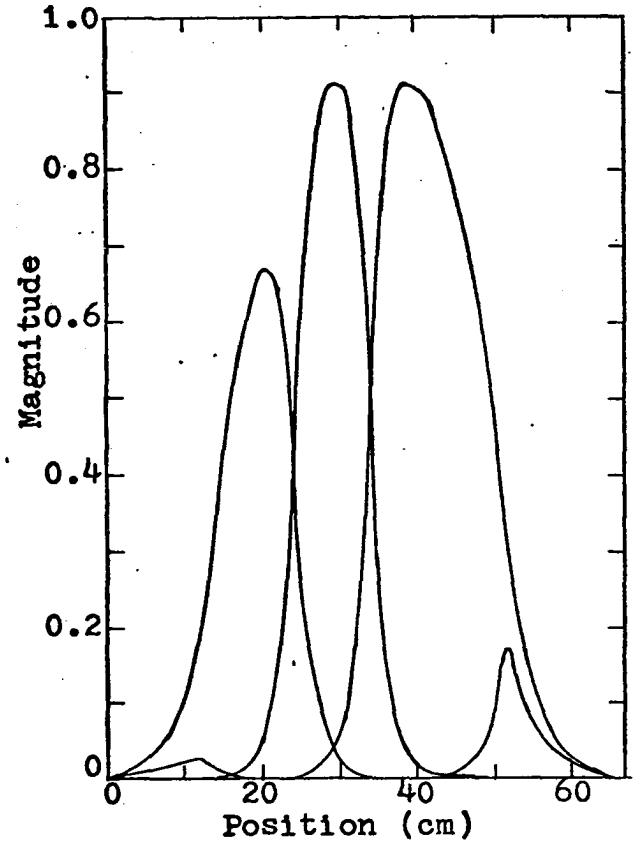

(b) Thermal adjoint modes

Figure III.14. Adjoint space modes for 5-MC2 analysis

$$\Sigma_{r10} = \Sigma_{r1}' - \Sigma_{r1}'' \qquad \text{where } \Sigma_{r1}' = 0.04 \text{ cm}^{-1}$$

and $$\Sigma_{r20} = \Sigma_{r2}' - \Sigma_{r2}'' \qquad \text{where } \Sigma_{r2}' = 0.015 \text{ cm}^{-1}.$$

This set of space functions and the adjoint space functions are shown in Figures III.13 and III.14.

The solutions obtained with this set of trial functions are shown in Figures III.15 and III.16. The exact solution and the solution obtained with the 5-M set of trial functions also are indicated. The asymptotic eigenvalue associated with this solution is 2254 sec^{-1}, which is slightly less than the 2271 sec^{-1} for the 5-M solution. However the 5-MC2 solution does yield better agreement with the exact solution than does the 5-M solution in the vicinity of the fuel-reflector interfaces. The solution in the left part of the perturbed region still disagrees with the exact solution, and this disagreement is difficult to remove using the present approach. However the trends which are indicated by the 5-MC2 results are of value to both the present study and to future applications.

In addition to the three sets of trial functions mentioned previously, a fourth set was also used to obtain an approximate solution to this problem. The source terms for this set, denoted by 5-MC3, were placed in the regions indicated in Figure III.17. It is to be noted that in this set the perturbed region was coupled to a fuel region and not a reflector region as were the other two sets of trial functions. The eigenvalues for this set of trial functions, along with

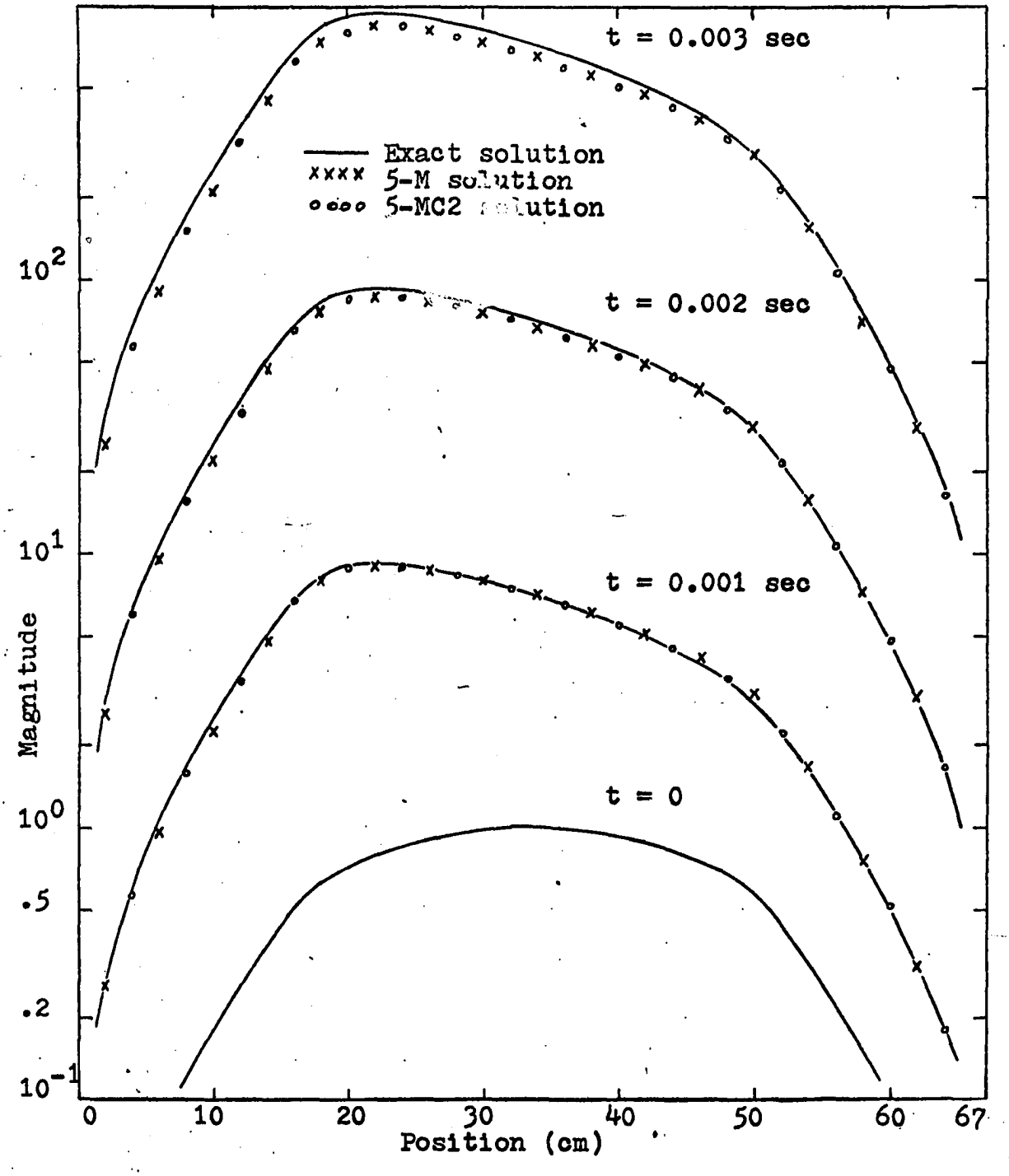

Figure III.15. Fast flux distribution, problem one

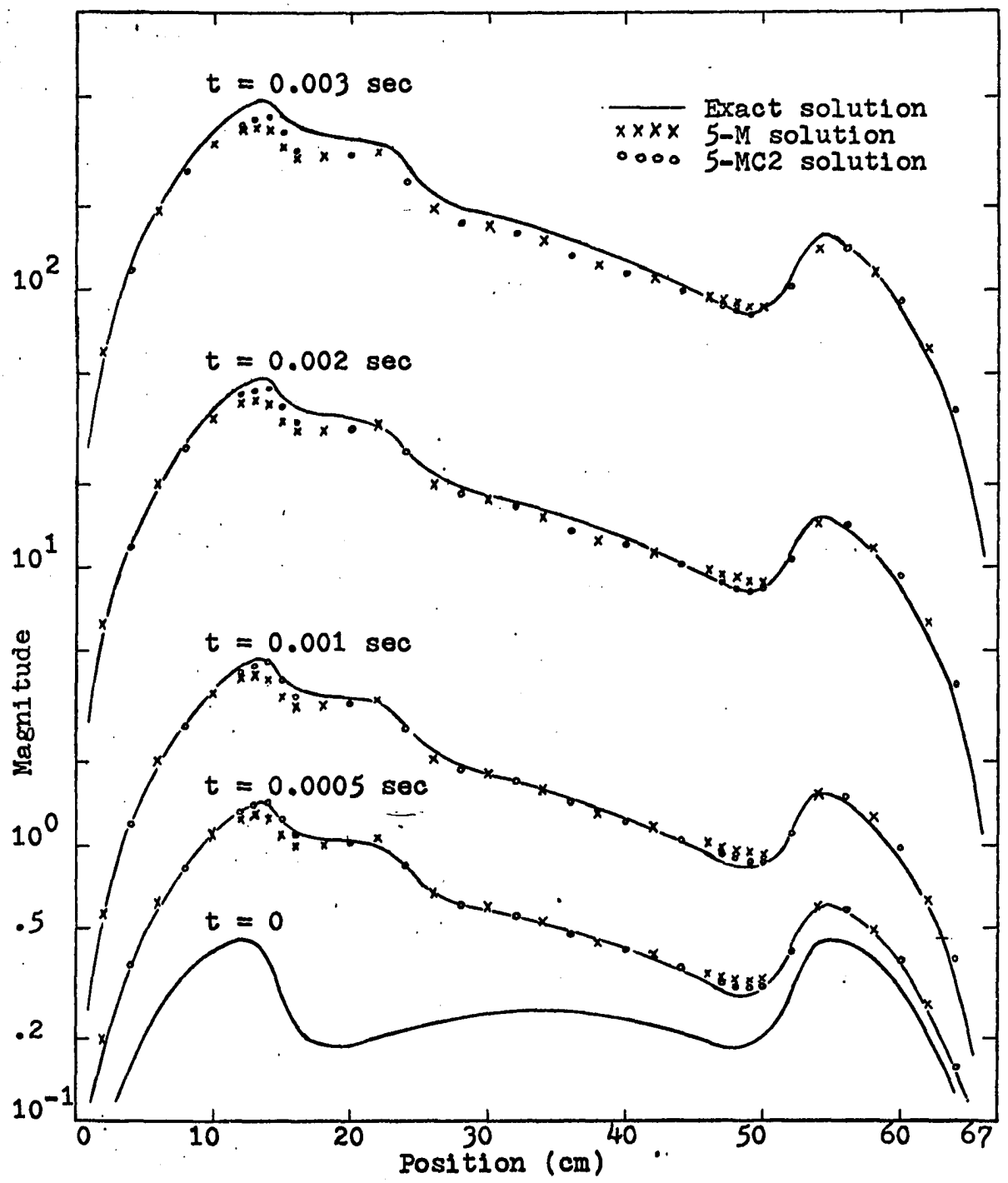

Figure III.16. Thermal flux distribution, problem one

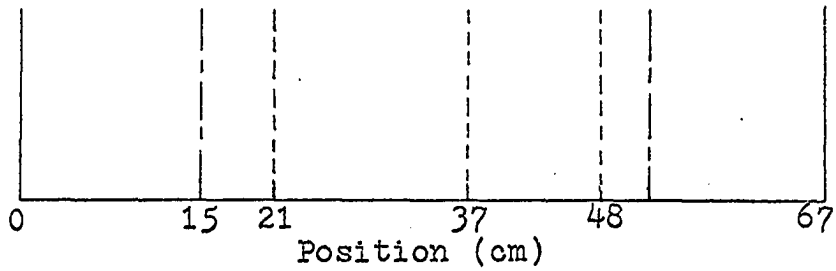

Figure III.17. Division of reactor for 5-MC3 analysis

the eigenvalues for the other sets and the exact asymptotic eigenvalue are given in Table III.1.

Table III.1. Eigenvalues for problem one

ν	ω_ν (sec^{-1})				
	Exact	5-M	5-MC1	5-MC2	5-MC3
1	2.308/3 *	2.271/3	2.137/3	2.254/3	1.963/3
2		-2.323/3	-2.387/3	-2.496/3	-2.570/3
3		-4.188/3	-5.763/3	-5.175/3	-5.290/3
4		-6.416/3	-1.000/4	-7.712/3	-9.433/3
5		-1.507/4	-1.596/4	-1.537/4	-1.528/4
6		-8.703/4	-8.723/4	-8.715/4	-8.703/4
7		-1.126/5	-1.140/5	-1.127/5	-1.139/5
8		-1.611/5	-1.671/5	-1.642/5	-1.627/5
9		-2.125/5	-2.587/5	-2.347/5	-2.508/5
10		-3.312/5	-4.157/5	-3.445/5	-3.612/5

* This notation means x 10^3

Information concerning the coupling of the space modes can be gleaned from the asymptotic eigenvalues. The smallest asymptotic eigenvalue was found for the 5-MC3 set of trial functions. The perturbed region in this case was coupled to a fuel region as opposed to the other cases of no coupling or

coupling to a reflector region. That this eigenvalue is the smallest is thought to result from the fact that coupling between the perturbed region and a fuel region has the effect of slowing down the solution since the coupling is between a region of low neutron removal and a region of greater neutron removal. This result should be especially true for a highly thermal model as is this particular reactor.

The next smallest eigenvalue is associated with the 5-MC1 set of trial functions. In this case the coupling is between a region of less removal (reflector region) and one of greater neutron removal (perturbed region). That the eigenvalue is still lower than the asymptotic eigenvalue can be explained by the fact that the entire reflector region is coupled to a part of the perturbed region. This would indicate a change in the flux shape across the entire reflector, a condition which does not physically occur.

The reason for the difference between the asymptotic eigenvalues for the 5-M and the 5-MC2 sets of trial functions is difficult to determine. These eigenvalues differ from the exact asymptotic eigenvalue by 1.60% (5-M) and by 2.34% (5-MC2).

It can be concluded from the time response curves and from the asymptotic eigenvalues that; (1) coupling in the region of the perturbation must be only between regions of large flux shape changes, (2) that this coupling should be between regions of low neutron removal (unperturbed region) and greater neutron removal (perturbed region), and (3) that

coupling away from the perturbed region can improve the solution near material interfaces.

B. Problem Two

The second problem studied was the time response of the reactor to a step change in the thermal group removal cross-section in the region $24 \leq x \leq 34$ (Figure III.18). A reactivity insertion of 2.78% $\delta k/k$ resulted from this perturbation. The exact solution was obtained by WIGLE with a time step of 5.0×10^{-6} sec.

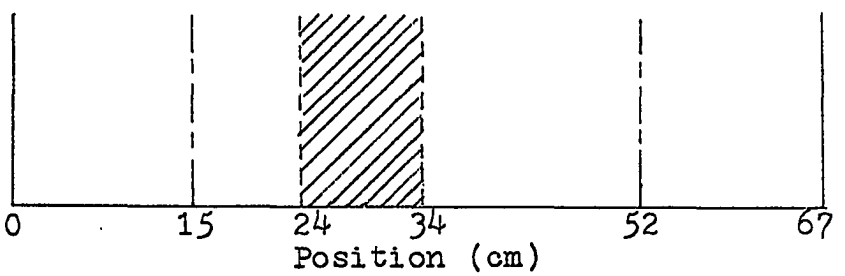

Figure III.18. Division of reactor for problem two —

Two sets of trial functions were employed to determine approximate solutions to this perturbation. The first set of trial functions was the 5-M set employed in the solution of the first problem in this study. The second set of trial functions, denoted by 4-MC, was made up of four space functions for each energy group.

The source term for the first mode was placed in the left reflector and part of the fuel region ($0 \leq x \leq 24$). The second mode was formed with the source term in the perturbed region ($24 \leq x \leq 34$), and the source term for the third mode

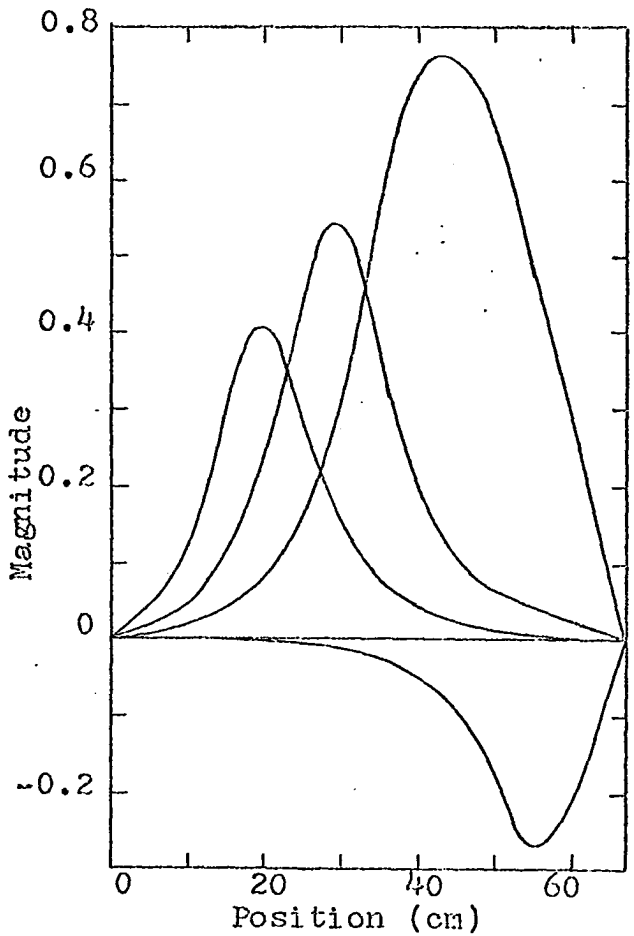

(a) Fast modes

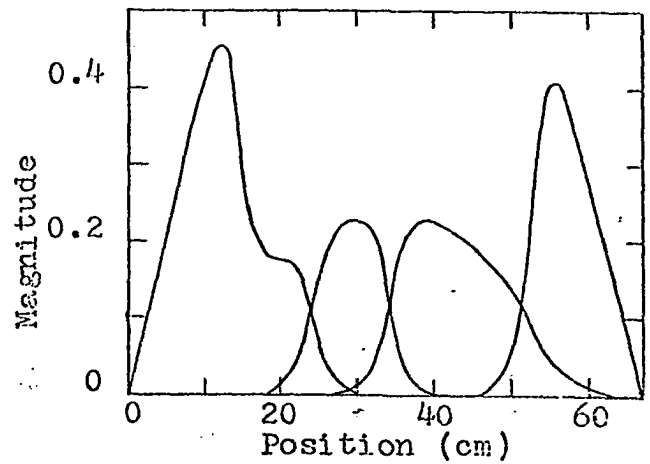

(b) Thermal modes

Figure III.19. Space modes for 4-MC analysis

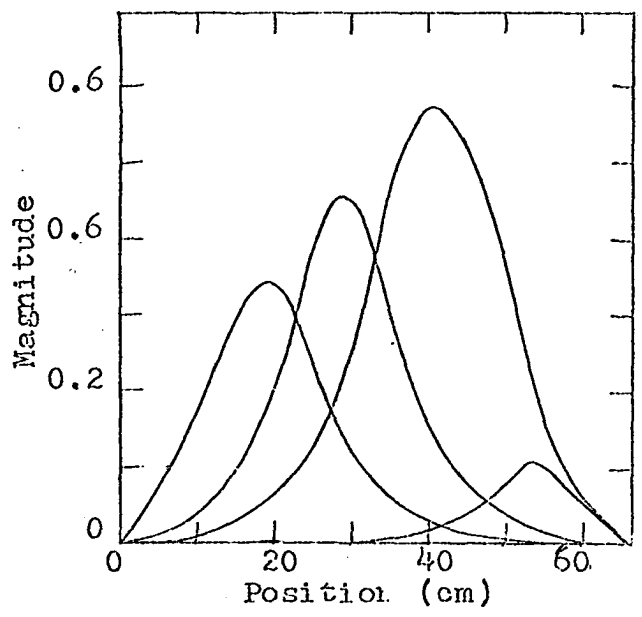

(a) Fast adjoint modes

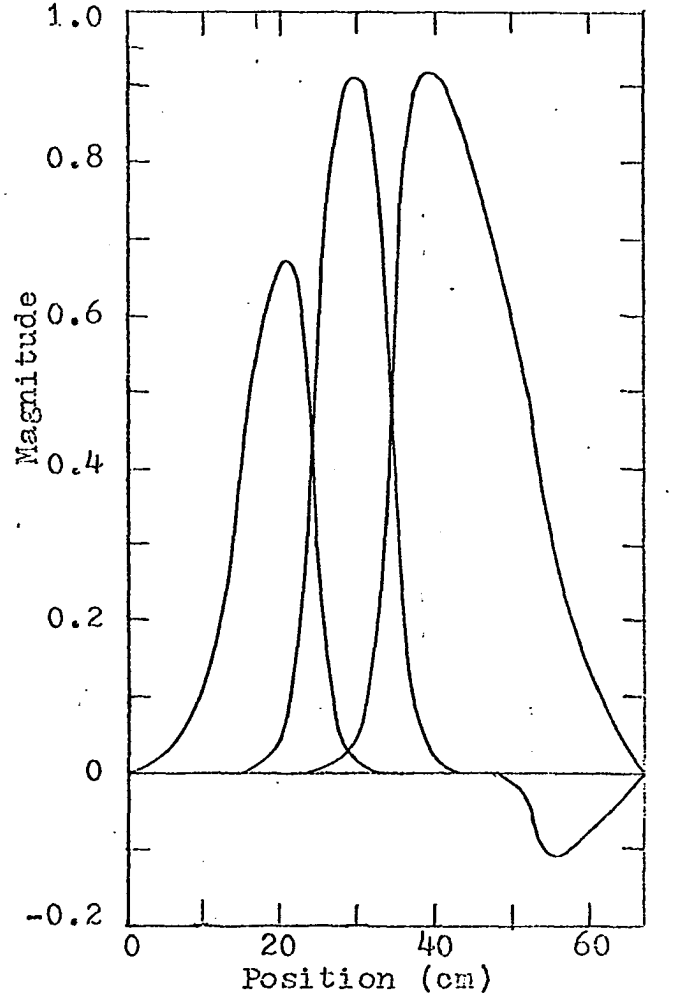

(b) Thermal adjoint modes

Figure III.20. Adjoint space modes for 4-MC analysis

was placed in the remaining part of the fuel ($34 \leq x \leq 52$). The source term for the fourth mode was placed in the right reflector. The space functions and the adjoint space functions are shown in Figures III.19 and III.20.

The flux distribution for the fast group is shown in Figure III.21 and for the thermal group in Figure III.22. The solutions obtained by the 5-M and the 4-MC sets of trial functions are shown along with the exact solution. The exact eigenvalue for this problem is 467.0 sec^{-1}. The asymptotic eigenvalue associated with the 5-M solution, 462.3 sec^{-1}, differed from the exact eigenvalue by 1.01% and the eigenvalue for the 4-MC solution, 460.1 sec^{-1}, differed from the exact eigenvalue by 1.48%.

The exact solution and the approximate solutions agree very well for the fast flux, the only difference due to the difference in the asymptotic eigenvalues. There is no difference in the two approximate solutions for the thermal flux except in the left reflector. The 4-MC solution slightly overestimates the exact solution because the mode for this reflector is coupled to a fuel region. The flux in the fuel subregion is increasing slightly faster than is the flux in the reflector. However the 4-MC solution does not differ, in terms of percent, from the exact solution any more than the 5-M solution differs from the exact solution.

It is to be noted that the solution to this problem cannot be obtained with less than five trial functions unless

coupled space functions are used. It also is noted that the two approximate solutions agree exactly in the fuel and right reflector regions, and only differ slightly in the left reflector region.

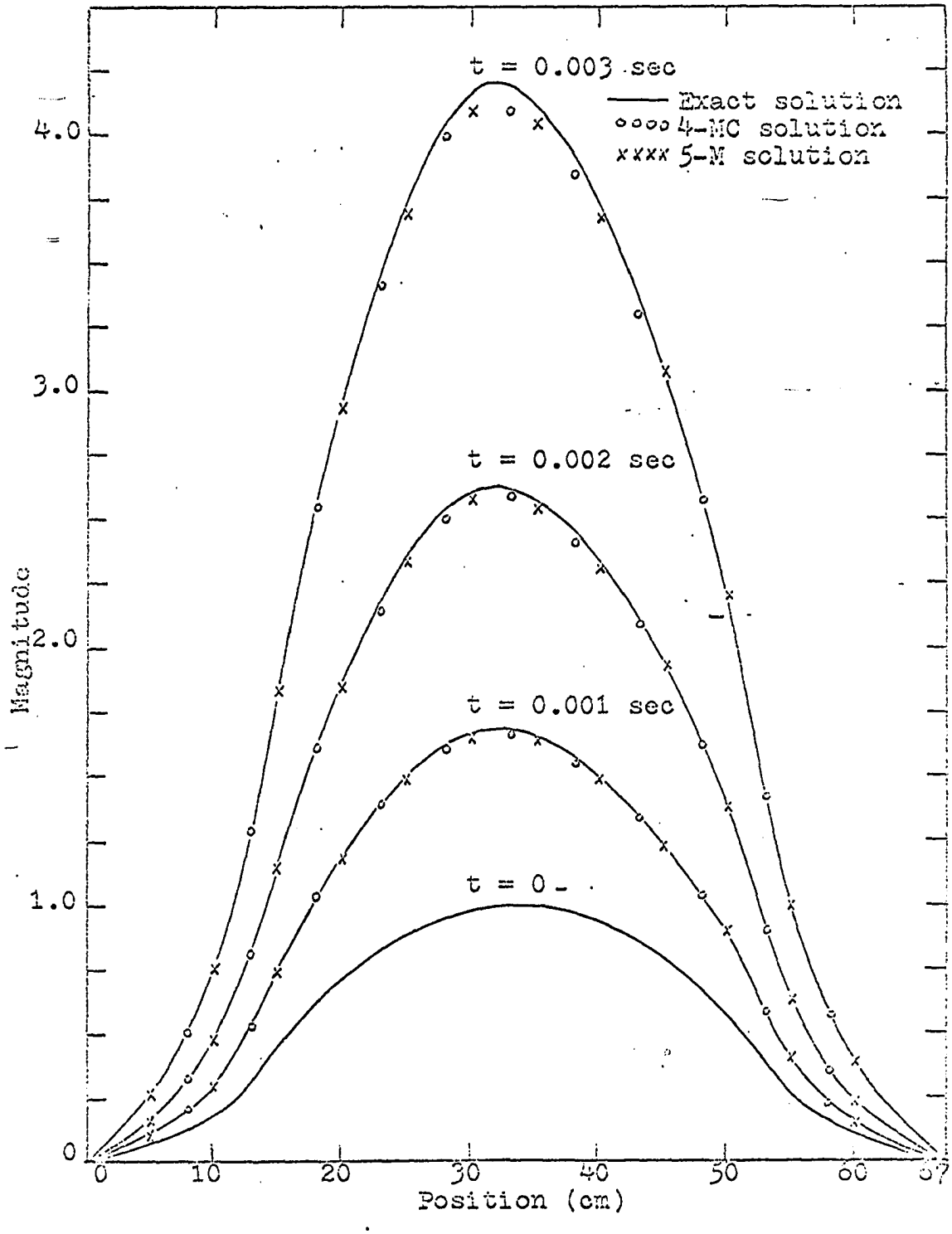

Figure III.21. Fast flux distribution, problem two

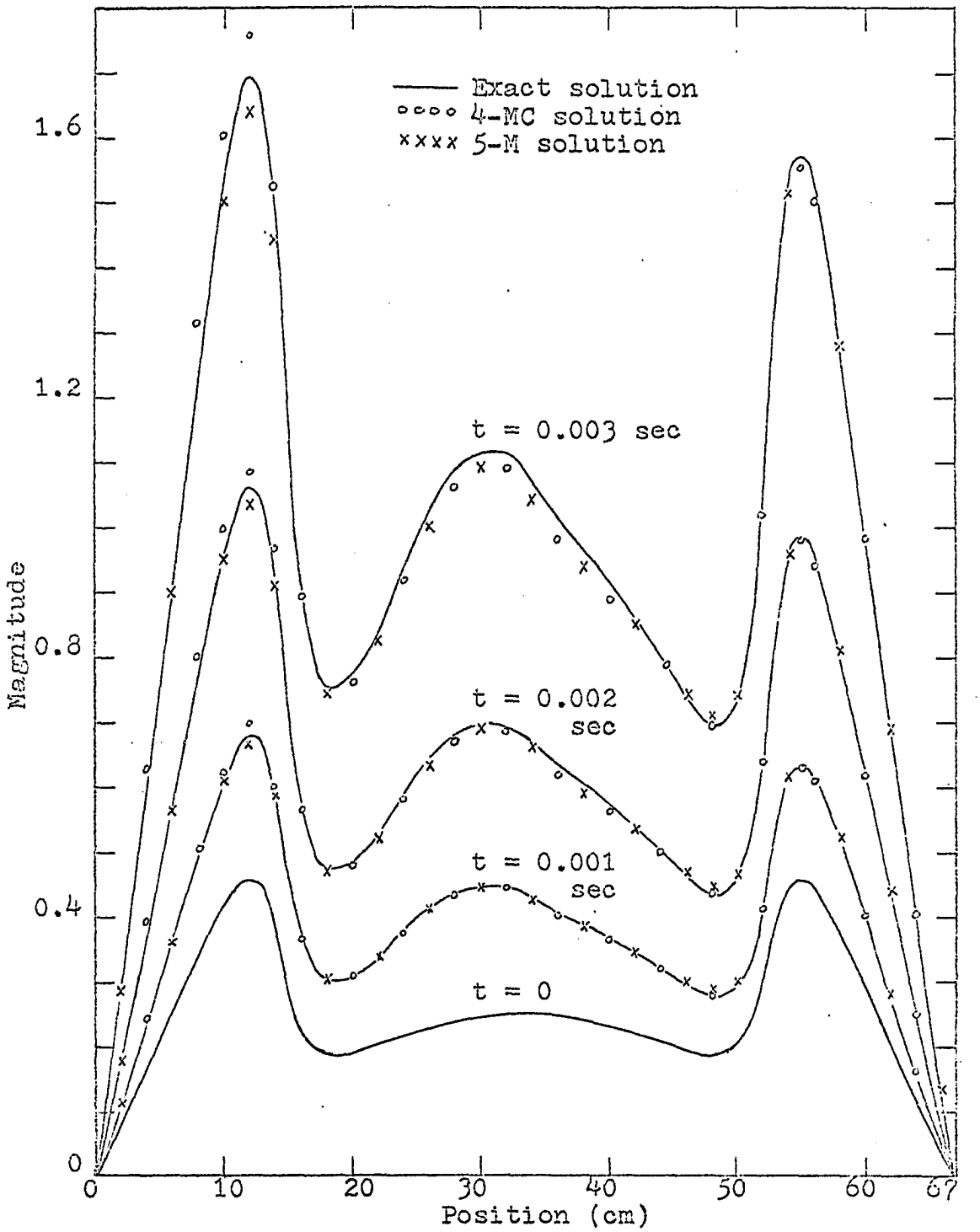

Figure III.22. Thermal flux distribution, problem two

IV. APPLICATION TO FREQUENCY RESPONSE

In this section the response of the reactor to a sinusoidal driving function will be determined. The driving function is formed by varying the thermal group removal cross-section about the steady state value. The response to this driving function (oscillator) is determined at various positions in the reactor. The frequency range investigated was from 10^{-2} radians/sec to 10^{5} radians/sec.

The oscillator was first placed in the center of the reactor and the response at this position was determined. The choice of this location for the oscillator and detector was made for two reasons. The first was to provide a comparison between the solutions reached with the Green's function modes and some other type of space functions, as the Green's function method has yet to be compared with another method.[1] In this case the other space functions are the Helmholtz modes as employed by Loewe (8). The location of the oscillator and detector at the center of the reactor permits some comparisons between the frequency response obtained by a space dependent method and the frequency response as determined by point reactor kinetics. This is the second reason for this choice of oscillator and detector location.

---

[1]Betancourt, J., Ames, Iowa. The space dependent frequency response of the reactor model used by Merritt (15) is being determined with trial functions employing the natural modes (9). Private communication. 1968.

In addition to the trial functions previously discussed with regard to the solution of the time dependent problem, two additional sets of trial functions were employed in the frequency response study. The first set, denoted by 3-MC, consisted of three trial functions for each energy group. The reactor was divided into source regions as shown in Figure IV.1. The first and third modes are formed by coupling the functions for the reflectors with the functions for the fuel region adjacent to the reflectors. These space modes and the adjoint space modes are shown in Figures IV.2 and IV.3.

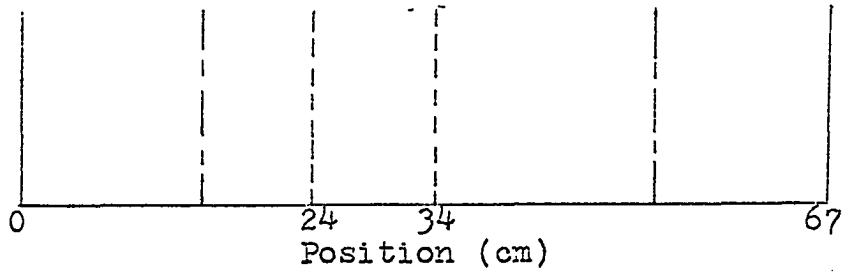

Figure IV.1. Division of reactor for 3-MC analysis

The second set of trial functions was chosen to provide a means of checking on the validity of the other approximate solutions. In contrast to the time dependent problem where an exact solution is available in the form of the WIGLE code, there is no available exact method of determining the frequency response. The common method for comparison of solutions is to increase the number of trial functions and check the solutions for convergence. While this method of comparison is not the best method, it is not without value.

The set of trial functions used for the purpose of

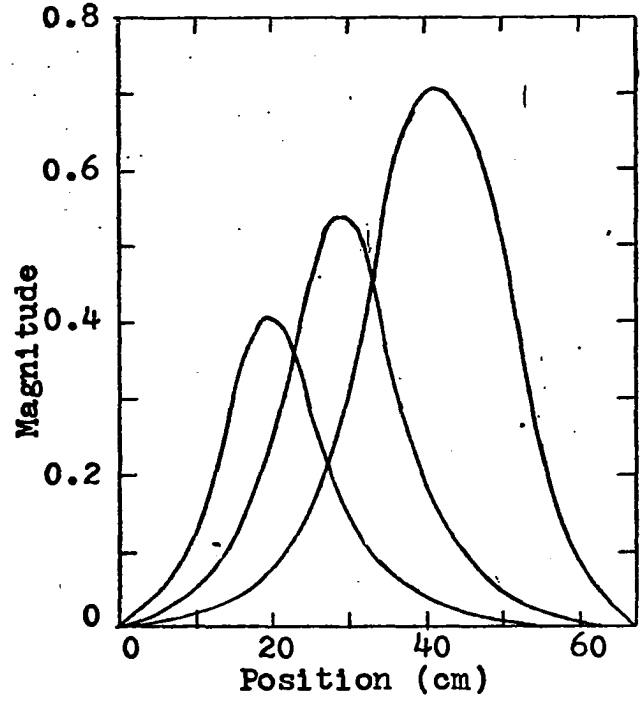

(a) Fast modes

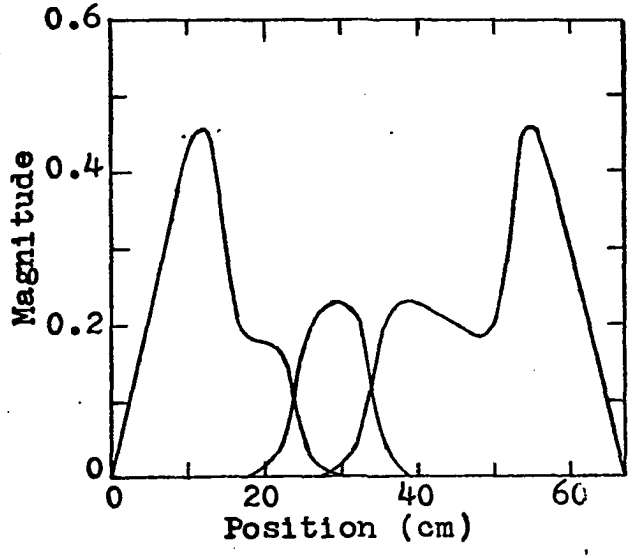

(b) Thermal modes

Figure IV.2. Space modes for 3-MC analysis

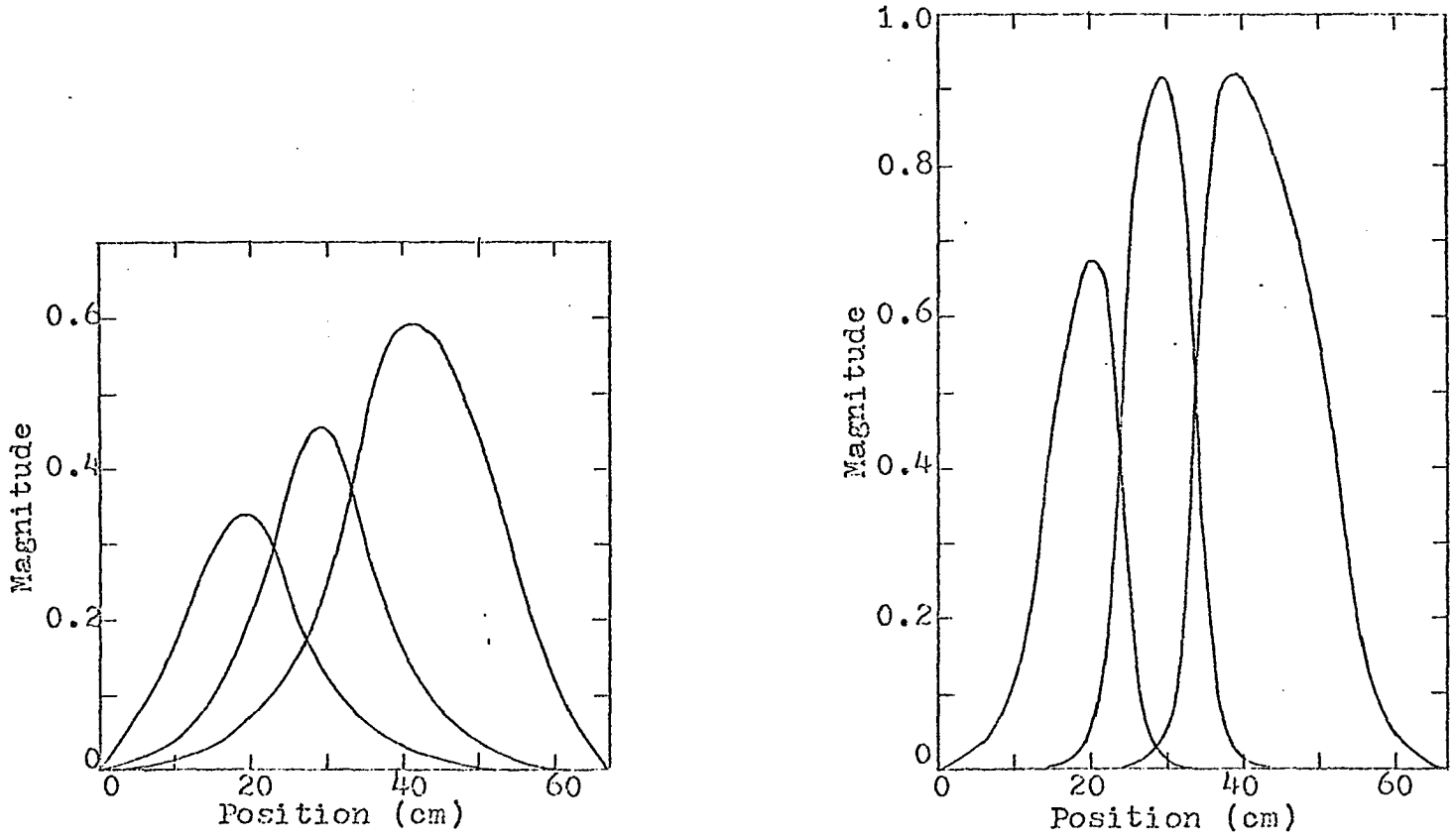

(a) Fast adjoint modes

(b) Thermal adjoint modes

Figure IV.3. Adjoint space modes for 3-MC analysis

comparison consisted of seven trial functions for each energy group. To obtain these space modes, the reactor was divided into regions as shown in Figure IV.4. The additional space modes were placed away from the oscillator as it is in these regions that space effects occur. The space functions and the adjoint space functions for this set of trial functions, denoted by 7-M, are shown in Figures IV.5 and IV.6.

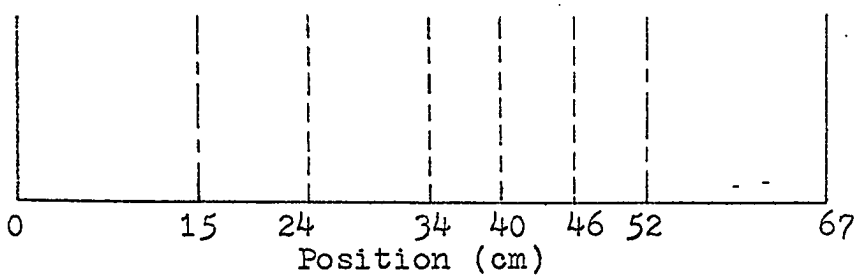

Figure IV.4. Division of reactor for 7-M analysis

The frequency response of the reactor with the oscillator and the detector in the center of the reactor is illustrated in Figures IV.7 and IV.8. In addition to the curves drawn for the 7-M, 5-M, and 3-MC analyses, selected points as presented by Loewe (8) are included. All the solutions for the magnitude of the frequency response agree very well over the entire frequency range considered. There is some disagreement between the phase solutions above 300 radians/sec, however this is very slight. The solutions obtained with the Green's function modes disagree with Loewe's solution in this region, but as all the Green's function solutions agree, it is difficult to say which is the correct solution. Loewe obtained the same results for both the reflected reactor and an equivalent

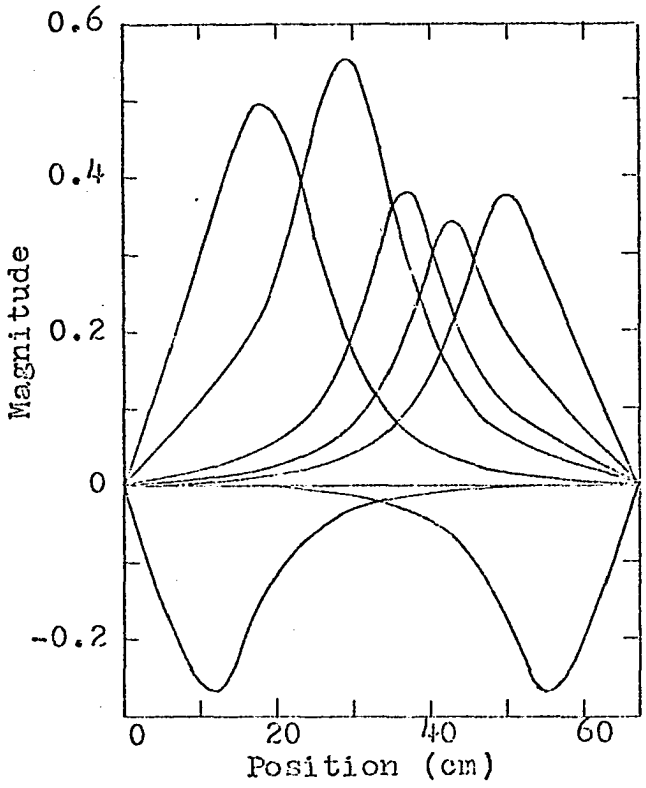

(a) Fast modes

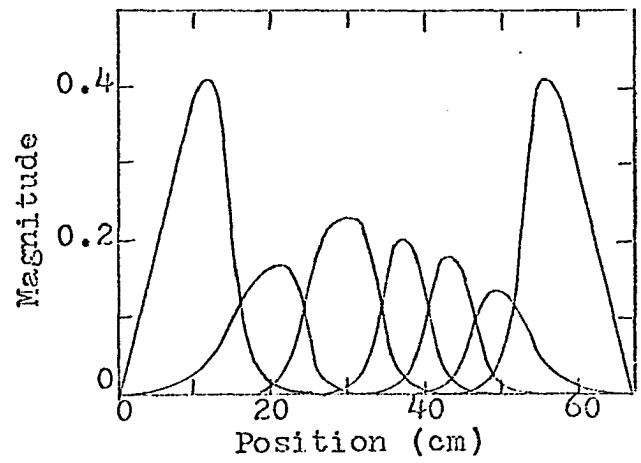

(b) Thermal modes

Figure IV.5. Space modes for 7-M analysis

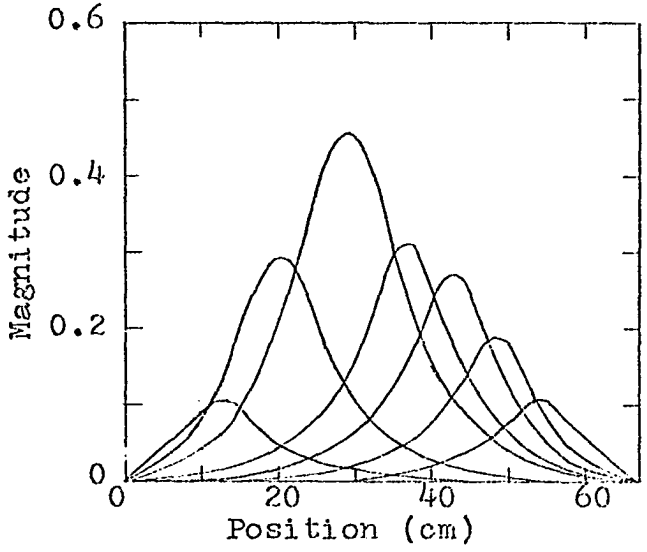

(a) Fast adjoint modes

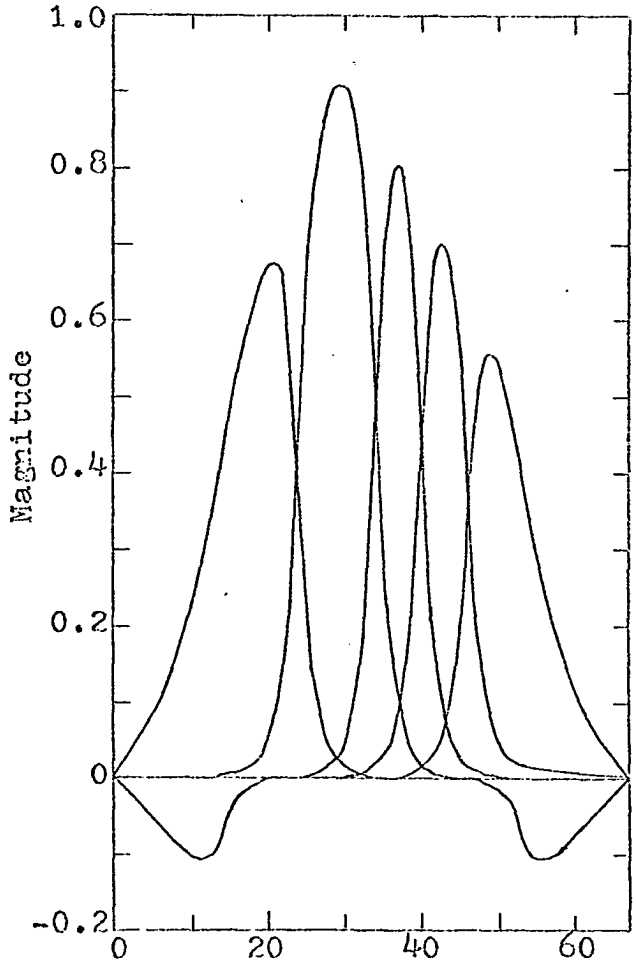

(b) Thermal adjoint modes

Figure IV.6. Adjoint space modes for 7-M analysis

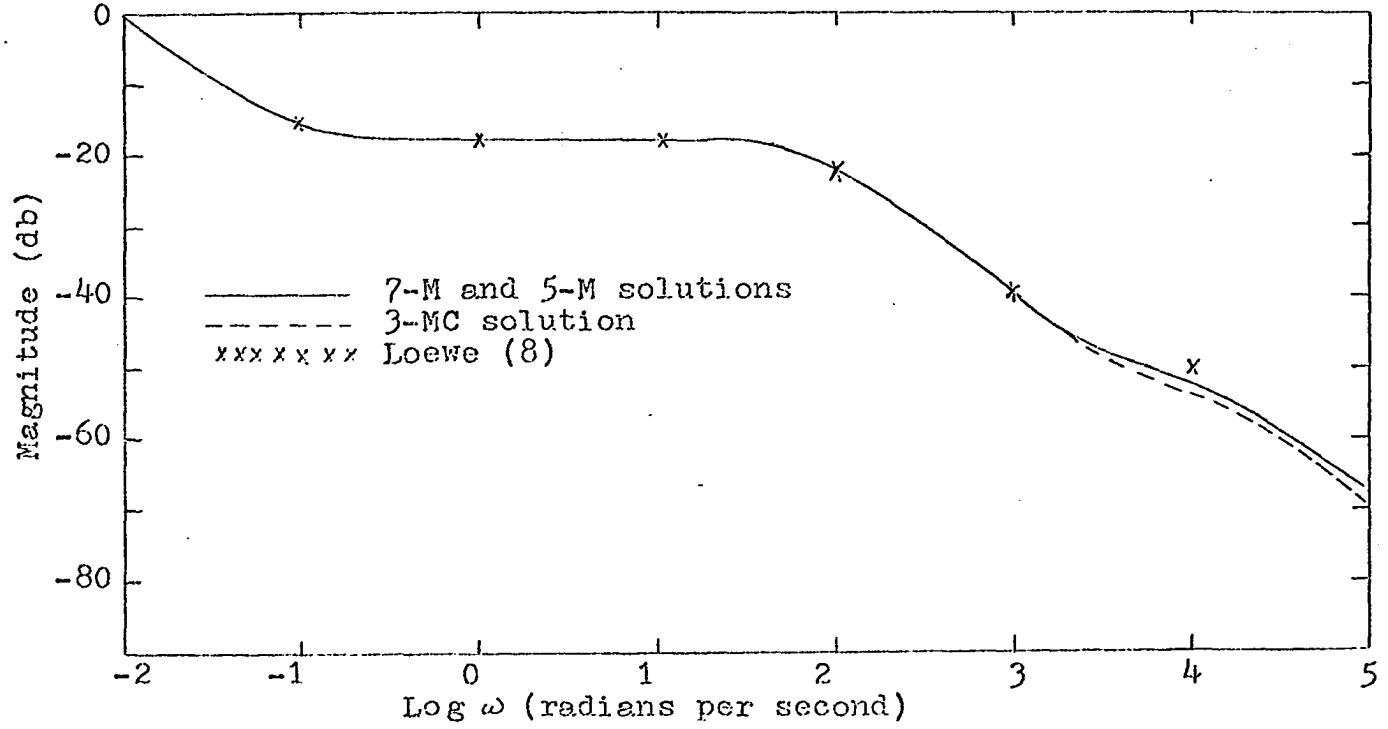

Figure IV.8. Magnitude of frequency response, oscillator at x = 33

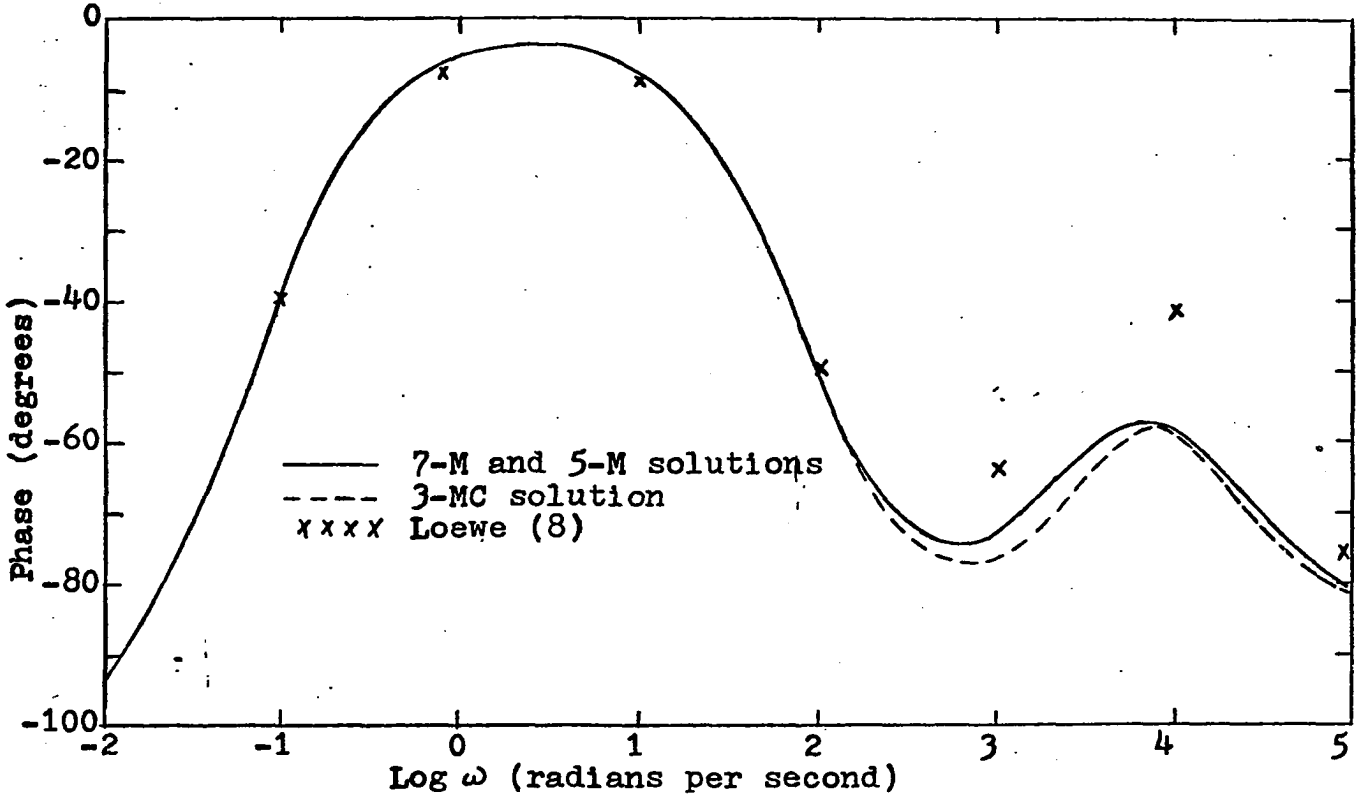

Figure IV.9. Phase of frequency response, oscillator at x = 33

bare reactor. Keaten and Griffin (29) found the same type of phase recovery at high frequencies as indicated in Figure IV.8 with a point reactor approach. They considered the neutrons returning to the fuel region from the reflector as an additional delayed neutron group.

One point to be considered in all the high frequency results is the applicability of the model. For the bare equivalent reactor, Loewe reported considerable differences between the diffusion equation solution and the telegrapher's equation solution for the phase response above 10^4 radians/sec. The difference in the solutions for the magnitude were slight and of no consequence.

In the second analysis the oscillator was placed in the left side of the fuel region at x = 19 and the response was determined at various positions in the reactor as indicated by Figure IV.10.

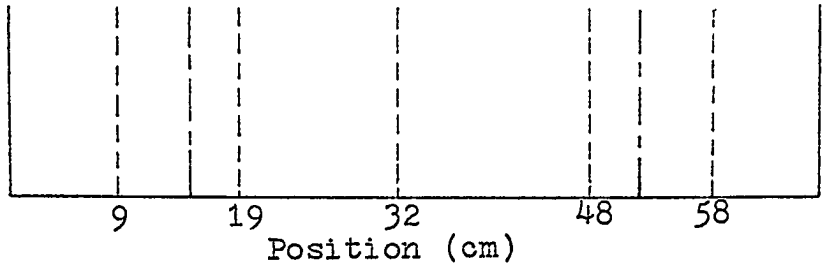

Figure IV.10. Detector locations for frequency analysis

A typical set of results is shown in Figures IV.11 and IV.12 for the 7-M analysis. Figure IV.11 indicates that there are no space effects on the magnitude of the frequency response below a frequency of 10^3 radians/sec. Above this

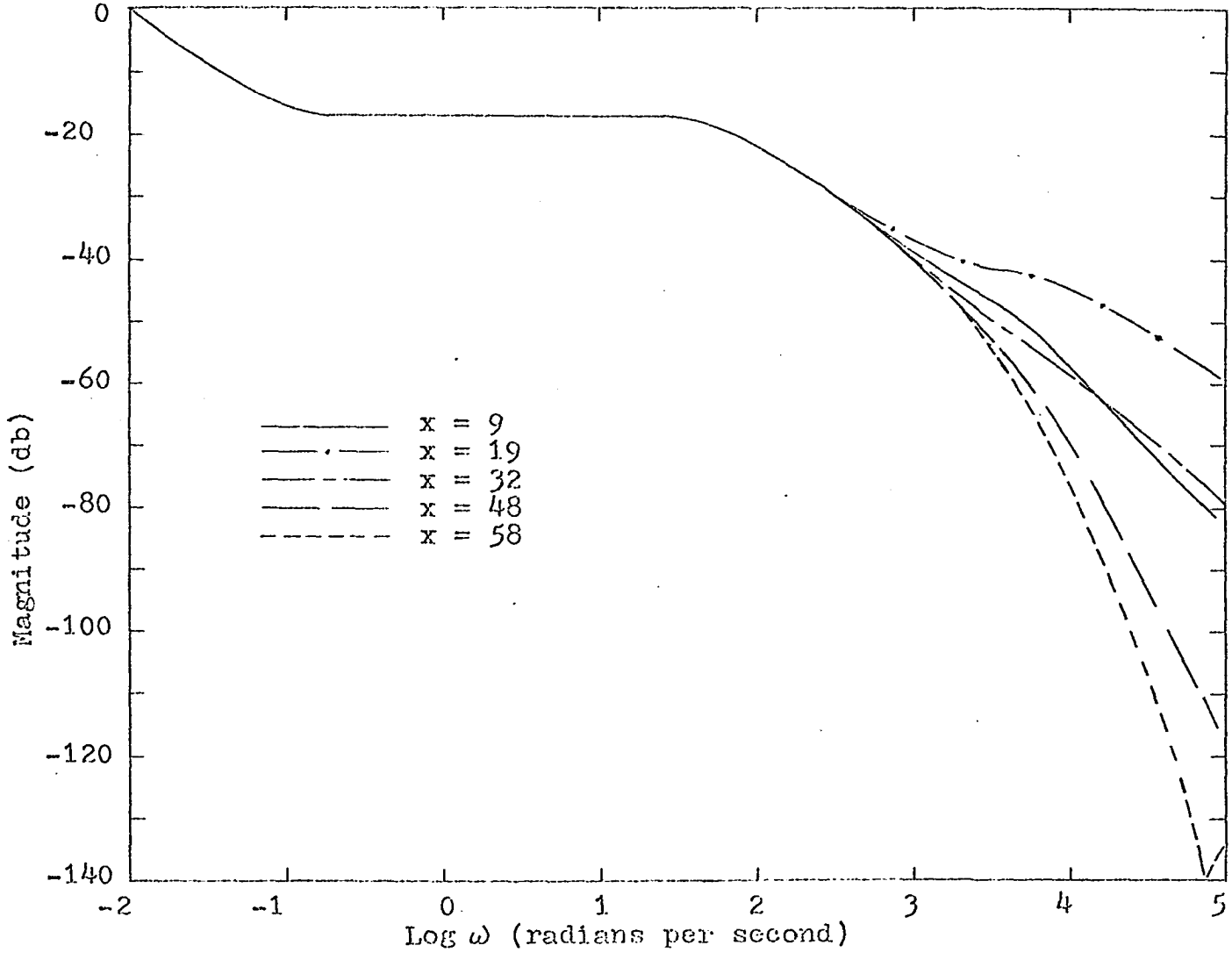

Figure IV.11. Magnitude of frequency response, oscillator at x = 19, 7-M solution

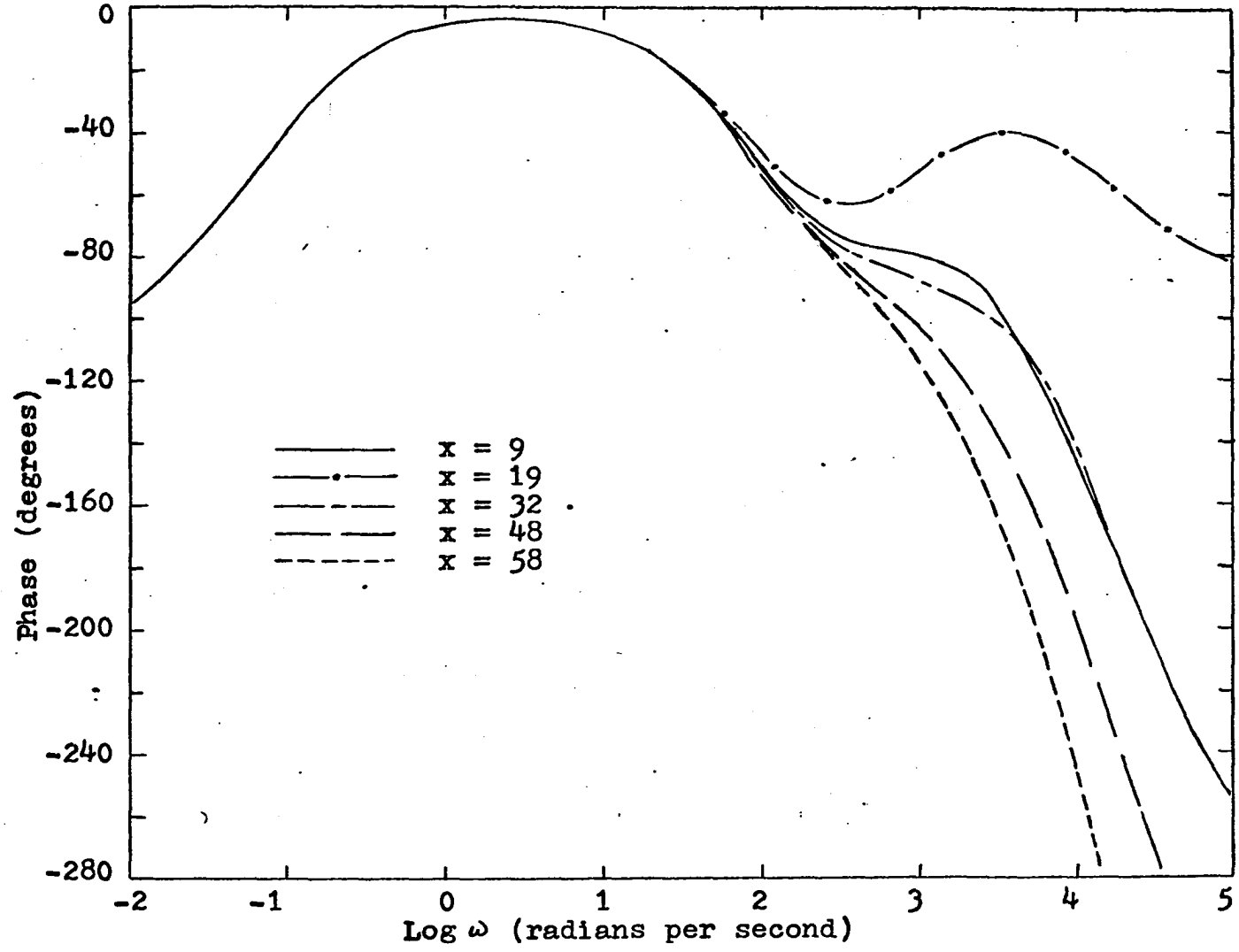

Figure IV.12. Phase of frequency response, oscillator at x = 19, 7-M solution

frequency the space effects become pronounced, especially at distances far from the oscillator as indicated by the solutions for the detector positions x = 48 and x = 58. At these positions the magnitude is greatly attenuated and the trends are the same as those reported by Foulke and Hansson (30) for a reflected reactor. It also is noted that the magnitude of the frequency response at x = 9 rises slightly in the vicinity of 3×10^3 radians/sec and then decreases. This initial rise is thought to be due to the proximity of the oscillator and the detector, with the difference in the material properties of the fuel and the reflector accounting for the change in slope at the frequency of 4×10^3 radians/sec.

The phase results shown in Figure IV.12 indicate that the phase response is more sensitive to space effects than is the magnitude of the frequency response. Away from the oscillator the phase decreases very rapidly above the β/ℓ breakpoint. With the detector and the oscillator in the same position the phase response is similar to the point reactor solution. The differences in the phase response for the detector locations x = 9 and x = 32 can be ascribed to the same causes as were the differences in the magnitude of the response for these two positions.

In an effort to gain a better understanding of the method of selecting the space modes for a frequency response analysis the response of the reactor at a given position is shown in Figures IV.13 to IV.22, with the different solutions chosen as

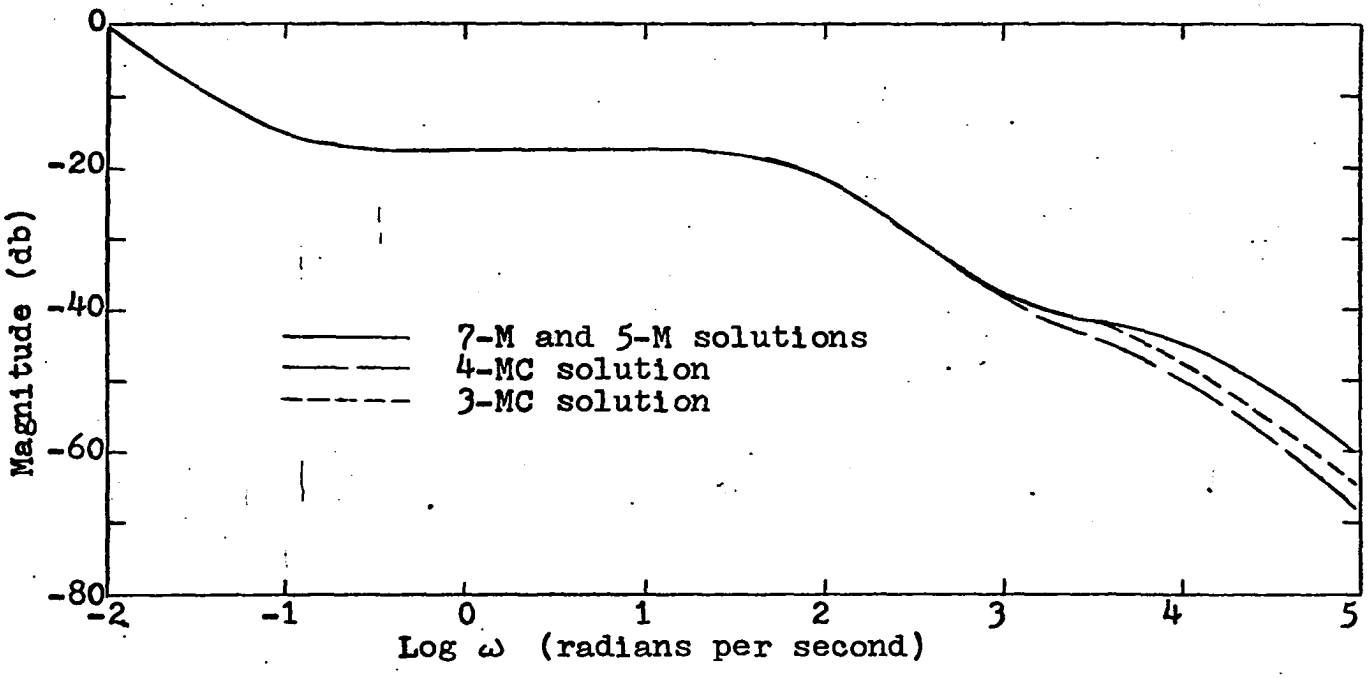

Figure IV.13. Magnitude of frequency response, detector at x = 19

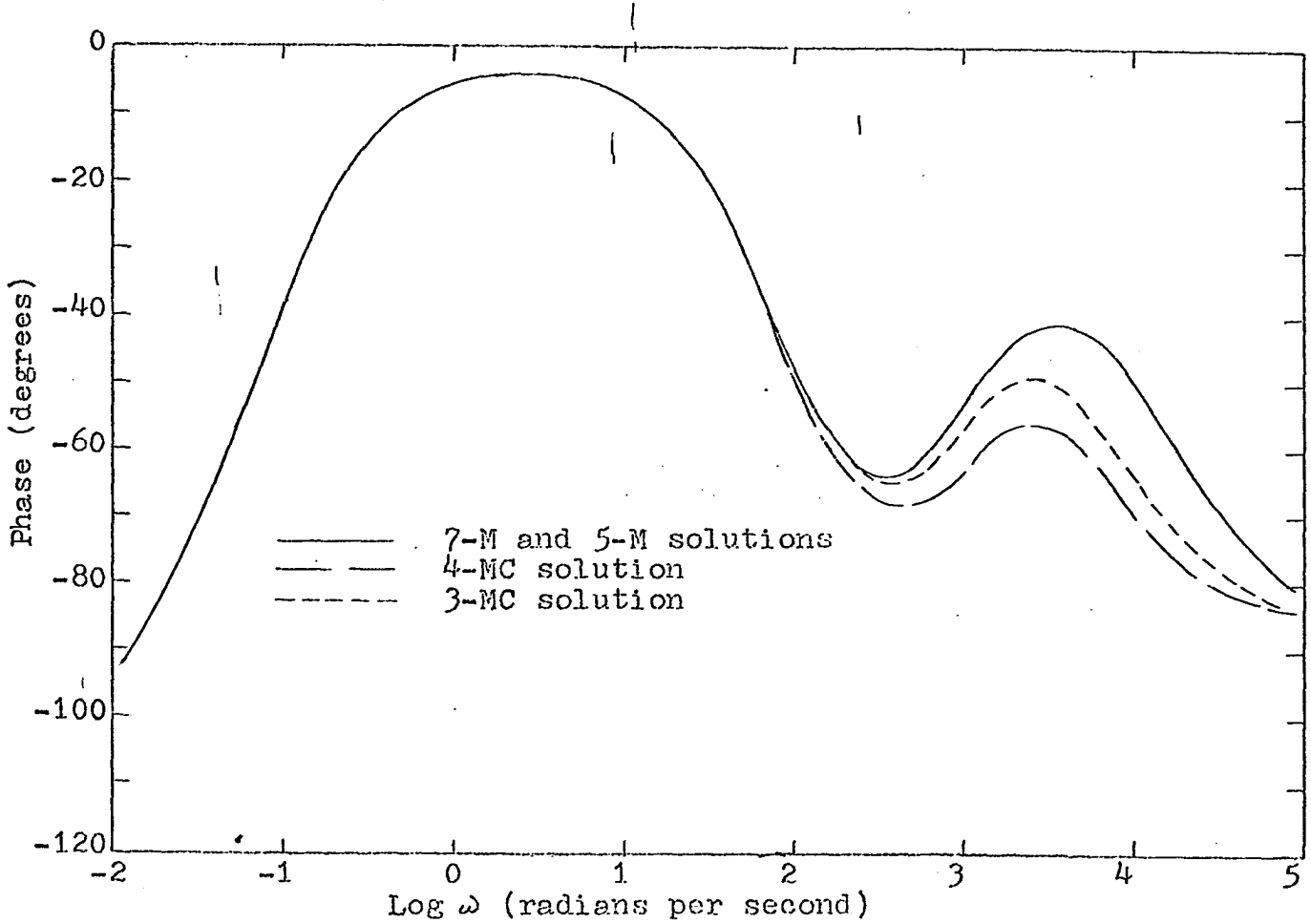

Figure IV.14. Phase of frequency response, detector at x = 19

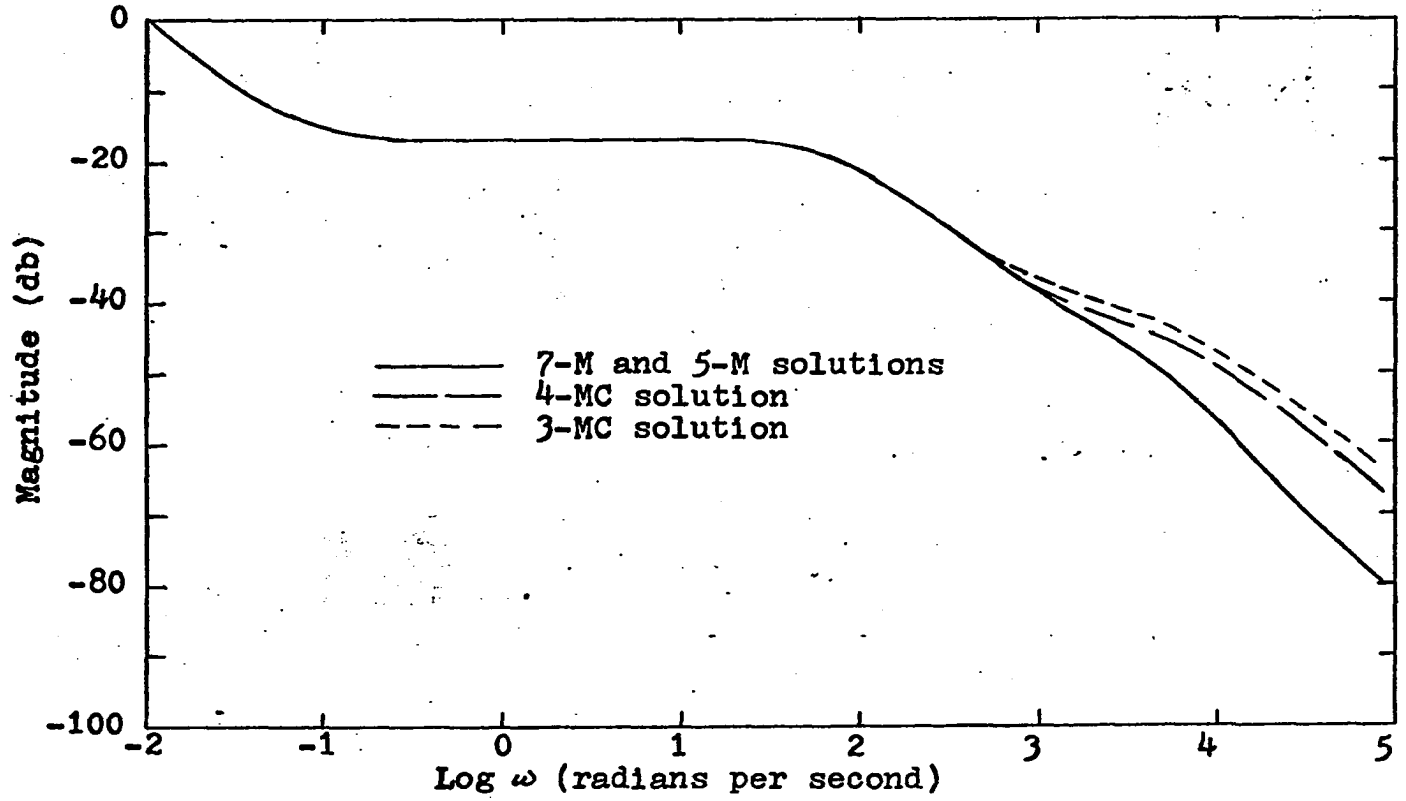

Figure IV.15. Magnitude of frequency response, detector at x = 9

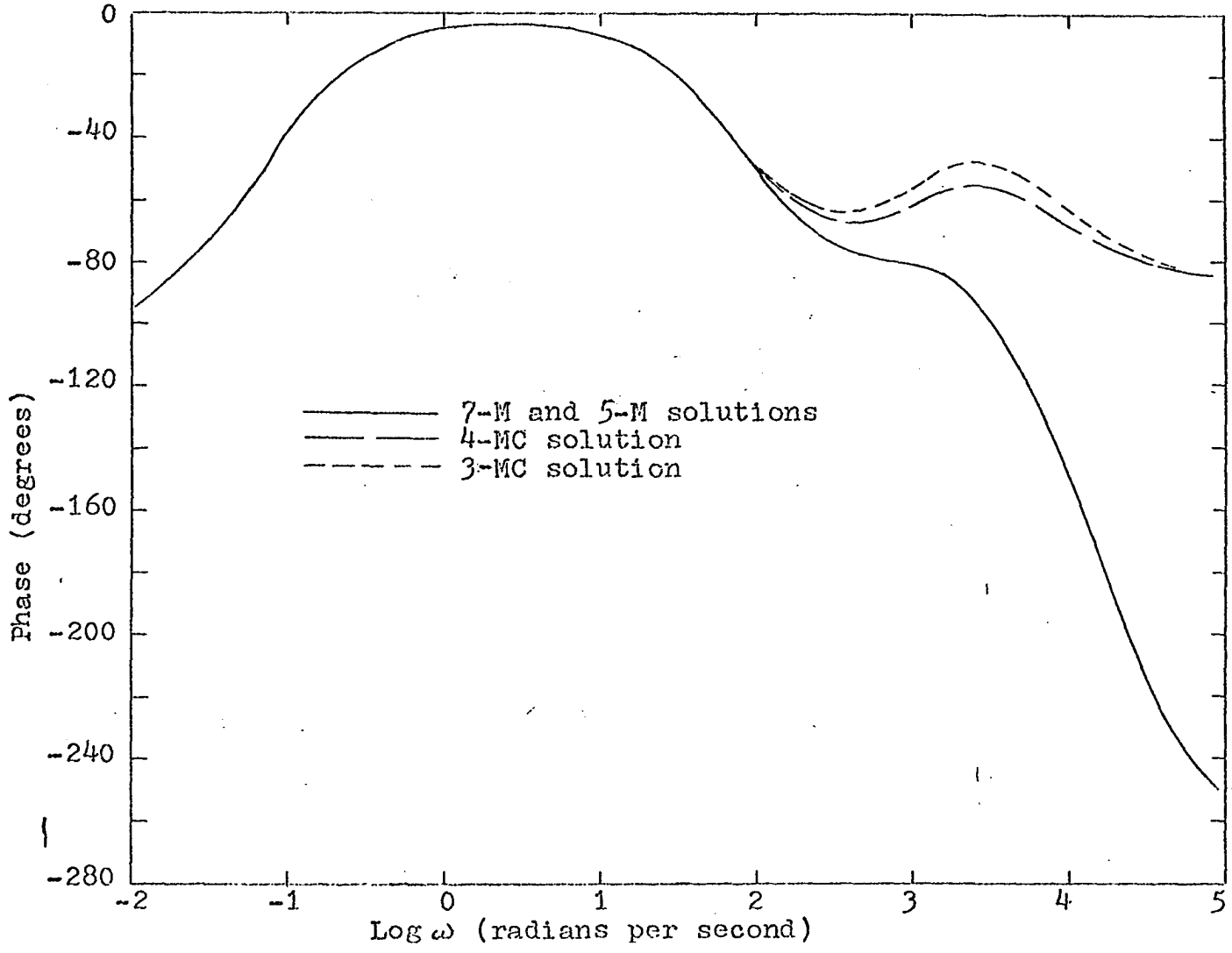

Figure IV.16. Phase of frequency response, detector at x = 9

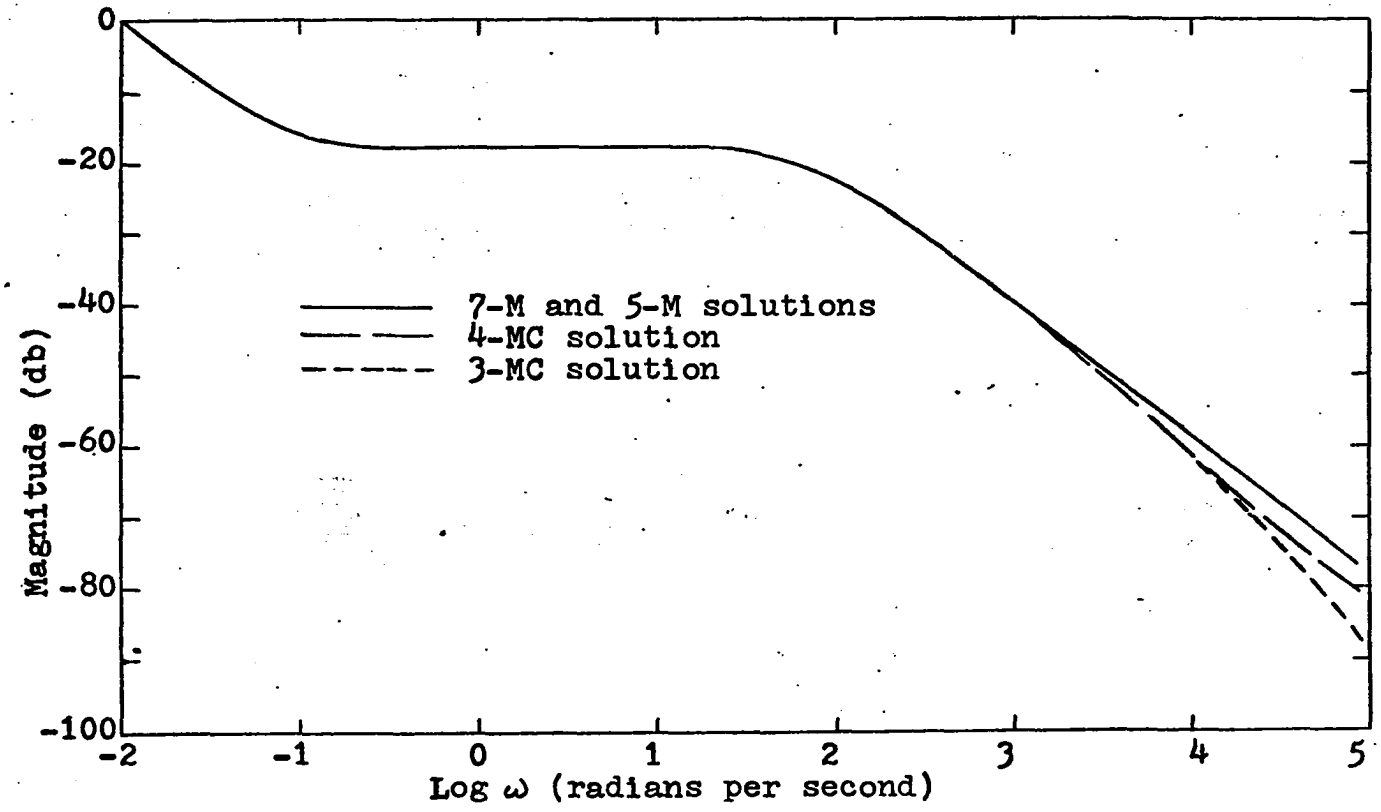

Figure IV.17. Magnitude of frequency response, detector at x = 32

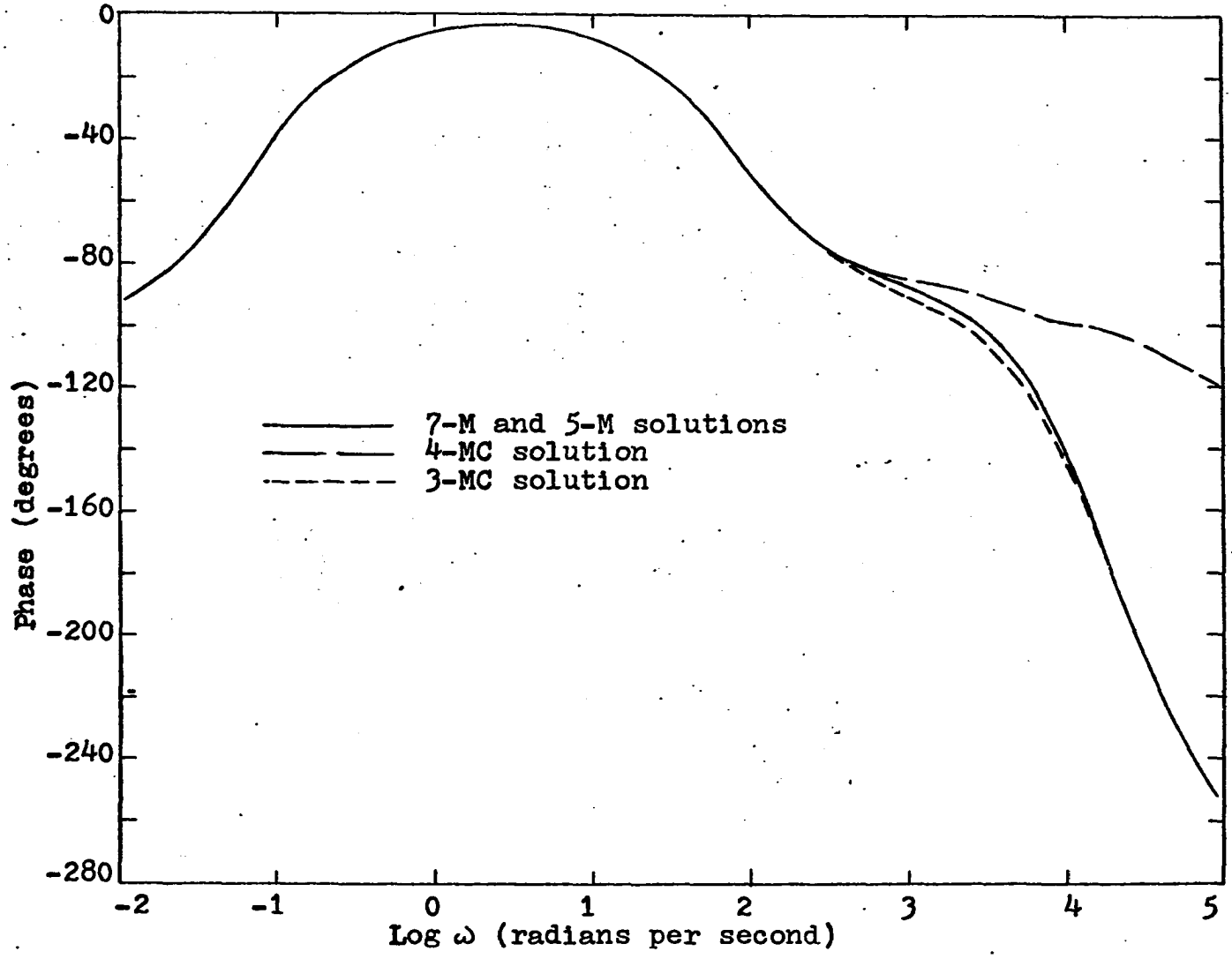

Figure IV.18. Phase of frequency response, detector at x = 32

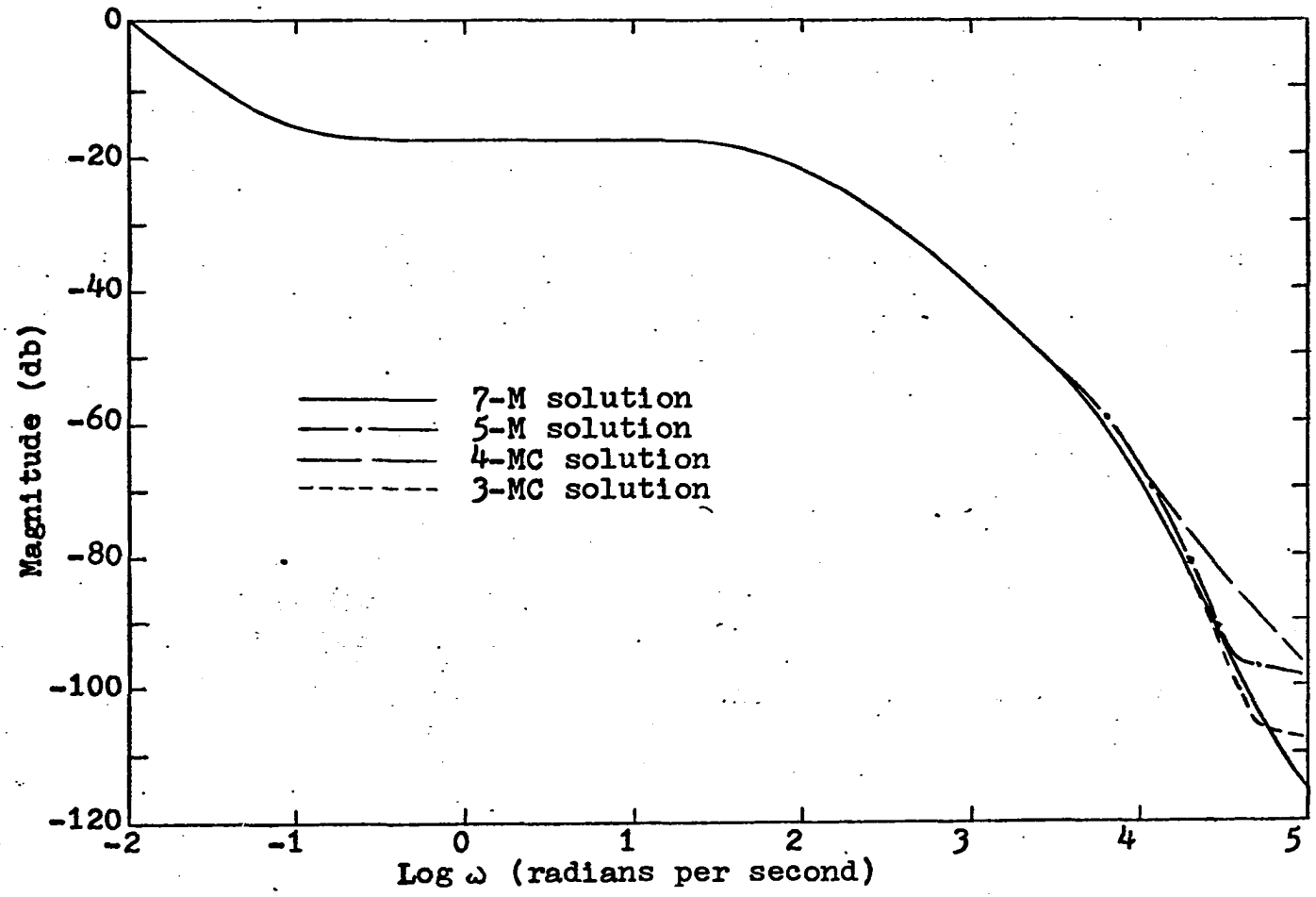

Figure IV.19. Magnitude of frequency response, detector at x = 48

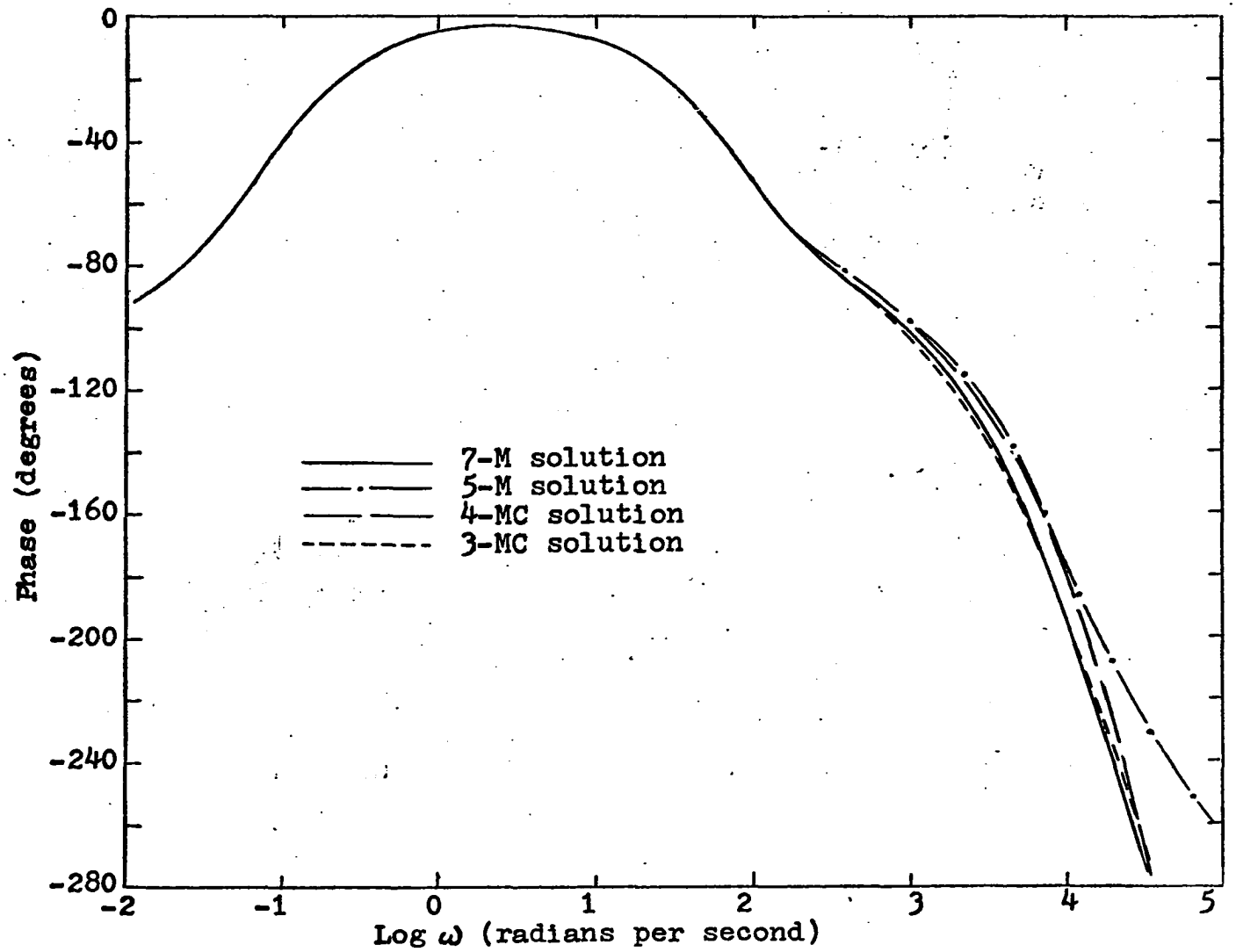

Figure IV.20. Phase of frequency response, detector at x = 48

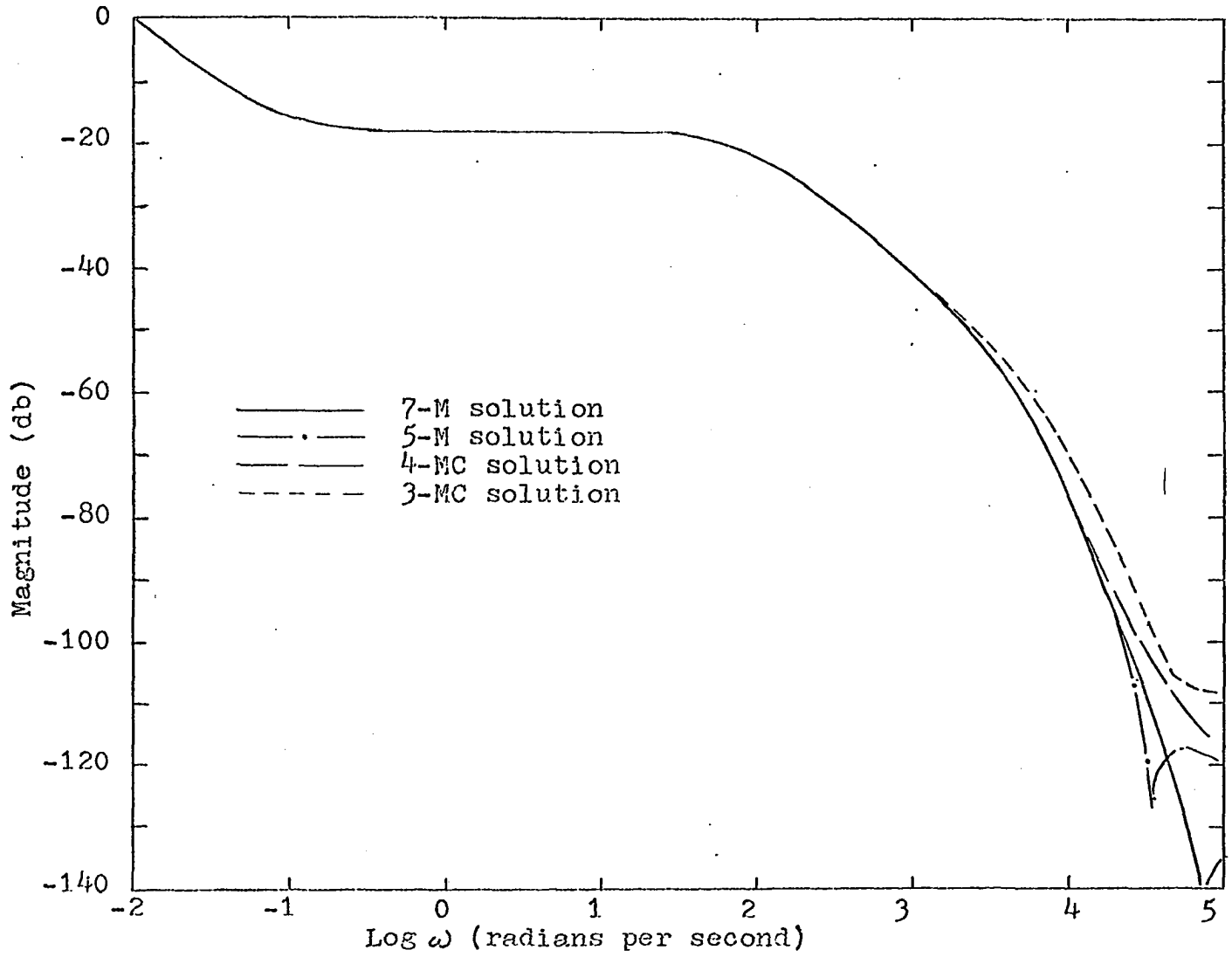

Figure IV.21. Magnitude of frequency response, detector at x = 58

Figure IV.22. Phase of frequency response, detector at x = 58

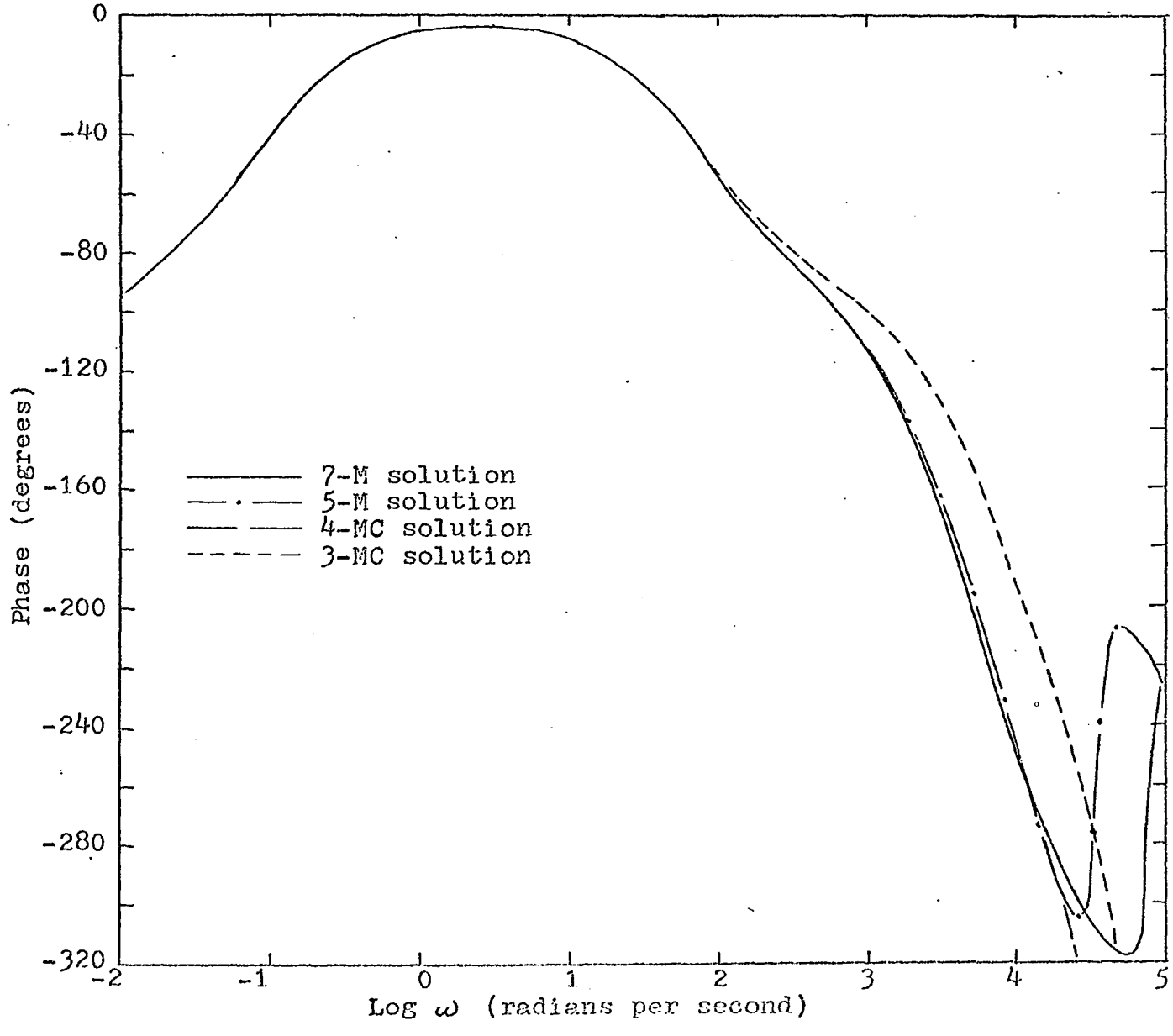
0
-40
-80
-120
-160
-200
-240
-280
-320
Phase (degrees)
-2
-1
0
1
2
3
4
5
Log ω (radians per second)
7-M solution
5-M solution
4-MC solution
3-MC solution

a parameter. The oscillator and detector were first placed in the same position (x = 19). The magnitude of the response given by the different solutions differs only slightly above 2×10^3 radians/sec with the greatest difference being only 6 db at 4×10^4 radians/sec. The 3-MC and 4-MC solutions show greater attenuation because the reflector and fuel modes are coupled in the left part of the reactor for these solutions. There are greater differences in the different phase response solutions, beginning at 10^2 radians/sec. These differences in this case are not considered to be critical to the solution since the same trends are indicated by all the solutions and there is no question as to the stability of the system.

Figures IV.15 and IV.16 show the magnitude and the phase of the response in the left reflector at x = 9. The differences in the magnitude solutions are more pronounced in this case than they were when the detector and oscillator were in the same position. The 7-M and 5-M solutions agree exactly for both the magnitude and phase response. However the 3-MC and the 4-MC solutions differ substantially. These solutions were obtained with the left reflector mode coupled to the fuel mode, and the effect of this coupling is indicated by these solutions. As in the time dependent studies, the less dispersive subregion tends to dominate the solution.

The solutions for the magnitude and the phase response at x = 32 are shown in Figures IV.17 and IV.18. There is very

little difference between the magnitude solutions except at very high frequencies where the 3-MC solution is being attenuated more rapidly than are the other solutions. The phase solutions agree very well except for the 4-MC solution. The reason for the extreme disagreement between the 4-MC solution and the other solutions is not known, especially since the magnitude solutions show good agreement.

As the detector is moved further from the oscillator, the differences in the solutions become more pronounced at frequencies greater than 10^4 radians/sec. In the fuel region (x = 48) the solutions agree very well up to this frequency. Assuming the diffusion equation is an adequate model above this frequency, the solutions are dependent on the number of trial functions, indicating that the approximate solutions have not converged to the correct solution.

In the right reflector the 7-M, 5-M and 4-MC solutions give excellent agreement up to 10^4 radians/sec. The difference between these solutions and the 3-MC solution can be found in the fact that the 3-MC solution was obtained with trial functions which were coupled to fuel regions, while the other solutions were obtained with separate trial functions for the fuel region and the right reflector. The resonance effect which is obtained with the 7-M and 5-M solutions has been observed both experimentally (31) and analytically[1] (15)

[1]Betancourt, J., Ames, Iowa. Results obtained with the natural mode approximation. Private communication. 1968.

for a coupled core reactor, but has not been noted for a single core reactor. There is no adequate explanation for this effect, and its appearance in this model is to be suspected because of the high frequency at which it occurs.

The results presented for the various frequency response solutions indicate that the coupled mode method can be used to determine accurate solutions for selected detector locations. If the response of the reactor is desired only in certain regions, it is recommended that the other regions be coupled, as the computation time for the solution increases by approximately $2N^2$, where N is the number of trial functions per energy group.

V. SUMMARY AND CONCLUSIONS

In this dissertation, a calculus of variations technique was used to study the space-time and space-frequency dependence of a reflected slab reactor. The space trial functions were the Green's function modes, with some modifications.

With regard to the space-time dependent problem, it was found that separate modes for each region were not always necessary. It is possible to form one mode for two regions which have different nuclear properties, and under some conditions improve on the solution obtained with a set of trial functions formed by the separate region approach. If the perturbation is in one of these regions, the coupling should be between a region of low dissipation (non-multiplying) and one of higher dissipation (multiplying) as opposed to coupling between two multiplying regions. Away from the perturbed region the coupling should be weak (the more dissipative subregion should be much smaller than the less dissipative subregion) for large changes in flux shape. If the change in flux shape away from the perturbation is slight, the coupling may include a greater portion of the fuel subregion.

It also was demonstrated that the number of trial functions necessary to describe the solution adequately could be reduced by employing this coupling technique, especially in the case of a large perturbation. The solution in the

vicinity of material interfaces was improved by the coupled mode method without adding additional trial functions, which would be necessary if the separate region approach is used.

The concept of a positive mode in the non-multiplying regions was introduced. This positive mode removes the possibility of encountering discontinuous space trial functions when employing the coupled mode approach as used in this dissertation.

If a small perturbation is introduced, the necessity for a trial function in a non-multiplying region away from the perturbation is removed due to the fact that any flux change will be the result of diffusion into the external reflector at the same rate as in the steady state situation. If the flux shape does not change in the adjacent multiplying region, the asymptotic shape in the reflector will take the same form as the steady state distribution. This coupling may lead to a slight overestimate of the flux at its peak in the reflector, which must be considered for the particular problem at hand. In most instances this result will be negligible. It is to be noted that a reactor with N different material regions should be analysed with at least N + 1 trial functions.

With regard to the space-frequency problem, it was found that the frequency response for the oscillator and detector in the center of the reactor obtained by four sets of trial functions employing Green's function modes compared favorably with a 19 mode solution (8) in which the space functions were

Helmholtz modes. The four sets of Green's function modes were (1) three modes, including two coupled modes, (2) four modes, including one coupled mode, (3) five modes, none coupled, (4) seven modes, none coupled.

For frequencies below 10^4 radians/sec the magnitude of the frequency response was not greatly affected by the presence of coupled modes in the set of trial functions. The phase response solutions obtained by the sets of trial functions containing coupled modes did not agree with the solutions obtained by the sets with no coupling modes for some detector locations. This disagreement was most pronounced when the detector was located in the non-multiplying subregion where the coupling was employed, and only slight disagreement occured in the fuel subregions.

The solutions obtained with the detector in the fuel region were less sensitive to coupling, with the exception of the phase solution at one position for the 4-MC set of trial functions.

Depending on the particular problem to be studied, the coupled mode approach can be used to determine the frequency response of a reflected reactor for frequencies up to 10^4 radians/sec with little loss in accuracy and a great gain in computation time. It is recommended that a separate mode be placed in a non-multiplying region if the frequency response at a point in that region is desired.

VI. SUGGESTIONS FOR FUTURE STUDY

The following list is a presentation of possible topics of interest in the field of reactor kinetics which follow either directly from this dissertation or indirectly from study and discussions concerning the calculus of variations.

1. The use of discontinuous trial functions in time would be a distinct advantage to the present formulation involving the Green's function modes. This would be applicable for large perturbations during which the flux undergoes significant shape changes during the transient. It is suggested that the first use of these discontinuous trial functions would be to introduce them at time $t = t_o^+$ (initial condition on the time coefficient is zero) to gain some physical insight into both the problem and their use. They also could be introduced at any later time, which would be applicable in the case of a linear (ramp) perturbation.

2. An investigation of the effect of coupling modes between fuel regions and internal reflectors is suggested for the analysis of coupled-core reactors.

3. The results presented in the previous pages for the frequency response are to be taken with some reserve at high frequencies. For this reason it is suggested that the telegrapher's equation be employed to study the frequency response of both reflected reactors and the coupled-core reactor studied by Merritt (15) to ascertain the presence

and/or cause of the resonance effect which was observed in the frequency response of both reactors in the external reflector away from the driving function.

4. The variational principles employed in reactor kinetics to date all depend on the inclusion of the adjoint problem for their success. Since the solution to the adjoint problem is not required for the solution of the diffusion problem, these principles actually yield more information than is necessary, at the same time requiring additional computational effort. For this reason it is suggested that some other type of variational principle be applied to the neutron diffusion problem. One such principle, introduced by Gurtin (32), is for initial-value problems, and has been applied to the heat conduction problem with some success (33). Another principle, introduced by Biot (34,35), utilizes a generalized thermal force which is found from a thermal potential and a dissipation function. This principle also has been applied to the heat conduction problem (36).

VII. ACKNOWLEDGEMENTS

The author wishes to express his appreciation to his major professors, Dr. Glenn Murphy and Dr. Richard Danofsky, for their interest during the preparation of this dissertation. The author also wishes to acknowledge Dr. Danofsky and fellow students for many interesting discussions and suggestions concerning both space-time neutron kinetics problems and the calculus of variations.

VIII. LITERATURE CITED

1. Hurwitz, H. The derivation and integration of the pile-kinetic equations. Nucleonics 5: 61-67. 1949.

2. Glasstone, S. and Edlund, M. C. The elements of nuclear reactor theory. New York, N.Y., D. Van Nostrand Co., Inc. 1952.

3. Weinberg, A. M. and Wigner, E. P. The physical theory of neutron chain reactors. Chicago, Ill., The University of Chicago Press. 1958.

4. Henry, A. F. The application of reactor kinetics to the analysis of experiments. Nuc. Sci. and Eng. 3: 52-70. 1958.

5. Henry, A. F. and Curlee, N. J. Verification of a method for treating neutron space-time problems. Nuc. Sci. and Eng. 4: 727-744. 1958.

6. Avery, R. Theory of coupled reactors. Second International Conference on the Peaceful Uses of Atomic Energy. 12: 182-191. New York, N.Y., United Nations. 1958.

7. Foderaro, A. and Garabedian, H. L. A new method for the solution of group diffusion equations. Nuc. Sci. and Eng. 8: 44-52. 1960.

8. Loewe, W. E. Space-dependent effects in the response of a nuclear reactor to forced oscillations. Nuc. Sci. and Eng. 21: 536-549. 1965.

9. Kaplan, S. The property of finality and the analysis of problems in reactor space-time kinetics by various modal expansions. Nuc. Sci. and Eng. 9: 357-361. 1961.

10. Foulke, L. R. and Gyftopoulos, E. P. Application of the natural mode approximation to space-time reactor problems. Nuc. Sci. and Eng. 30: 419-435. 1967.

11. Harris, D. R., Kaplan, S. and Margolis, S. G. Modal analysis of flux tilt; transients in a nonuniform-reactor. Am. Nucl. Soc. Trans. 2: 178-179. 1959.

12. Dougherty, D. E. and Shen, C. N. The space-time neutron kinetic equations obtained by the semi-direct variational method. Nuc. Sci. and Eng. 13: 141-148. 1962.

13. Carter, N. E. and Danofsky, R. A. The application of the calculus of variations and the method of Green's function to the solution of coupled core kinetics equations. In Chezem, C. G. and Kohler, W. H., editors. Conf. Coupled Reactor Kinetics, College Station, Texas, Jan. 1967. Pp. 249-269. College Station, Texas, The Texas A and M Press. 1967.

14. Carter, N. E. Solution of space-time kinetic equations for coupled core nuclear reactors. Unpublished Ph.D. thesis. Ames, Iowa, Library, Iowa State University of Science and Technology. 1967.

15. Merritt, I. W. Spatially dependent frequency response of coupled core reactors. Unpublished Ph.D. thesis. Ames, Iowa, Library, Iowa State University of Science and Technology. 1968.

16. Yasinsky, J. B. On the application of time-synthesis techniques to coupled core reactors. Nuc. Sci. and Eng. 32: 425-429. 1968.

17. Kaplan, S. and Bewick, J. A. Space and time synthesis by the variational method. U.S. Atomic Energy Commission Report WAPD-BT-28 (Westinghouse Electric Corp. Atomic Power Division, Pittsburg, Pa.). 1963.

18. Yasinsky, J. B. On the application of time-synthesis techniques to coupled-core-type reactors. Am. Nucl. Soc. Trans. 10: 570-571. 1967.

19. Yasinsky, J. B., Lynn, L. L., Kaplan, S., and Porsching, T. A. A combined space-time synthesis model-numerical comparisons with exact two-group two dimensional transient solutions. Am. Nucl. Soc. Trans. 11: 172-173. 1968.

20. Kantorovich, L. V. and Krylov, V. I. Approximate methods of higher analysis. New York, N.Y., Interscience Publishers, Inc. 1958.

21. Morse, P. M. and Feshbach, H. Methods of theoretical physics. Part I. New York, N.Y., McGraw-Hill Book Company, Inc. 1953.

22. Lewins, J. The approximate separation of kinetics problems into time and space functions by a variational principle. J. Nuc. Energy 12, Part A: 108-112. 1960.

23. Lewins, J. Importance: the adjoint function. London, England, Pergamon Press, Ltd. 1965.

24. Pomraning, G. C. A variational description of dissipative processes. J. Nuc. Energy 20, Part A: 617-634. 1966.

25. Cadwell, W. R., Henry, A. F., and Vigilotti, A. J. WIGLE. A program for the solution of the two-group space-time diffusion equations in slab geometry. U.S. Atomic Energy Commission Report WAPD-TM-416 (Westinghouse Electric Corp. Atomic Power Division, Pittsburg, Pa.). 1964.

26. Radd, M. E. WIGLE-40, A two-group, time-dependent diffusion theory for the IBM-7040 computer. U.S. Atomic Energy Commission Report IDO-17125 (Phillips Petroleum Corp. Atomic Energy Division, Idaho Falls, Idaho). 1965.

27. Gill, S. A process for the step-by-step integration of differential equations in an automatic digital computing machine. Camb. Phil. Soc. Proc. 47: 96-108. 1951.

28. Kohler, W. H. Variational method for prompt neutron kinetics. Nukleonik 8: 203-215. 1966.

29. Keaten, R. W. and Griffin, C. W. Reflected reactor kinetics. U.S. Atomic Energy Commission Report NAA-SR-7263 (North American Aviation, Inc. Atomics International, Canoga Park, Calif.). 1963.

30. Hansson, P. T. and Foulke, L. R. Investigations in spatial reactor kinetics. Nuc. Sci. and Eng. 17: 525-533. 1963.

31. Hendrickson, R. A. Cross-spectral density measurements in a coupled-core reactor. Unpublished Ph.D. thesis. Ames, Iowa, Library, Iowa State University of Science and Technology. 1966.

32. Gurtin, M. E. Variational principles for linear initial-value problems. Quart. Appl. Math. 22: 252-256. 1964.

33. Leitman, M. J. and Gurtin, M. E. On the use of variational principles for the approximate solution of linear initial-value problems. Office of Naval Research Report NR-064-406 (Brown University, Division of Applied Mathematics, Providence, R.I.). 1964.

34. Biot, M. A. Thermoelasticity and irreversible thermodynamics. J. Appl. Phys. 27:240-253. 1956.

35. Biot, M. A. Further developments of new methods in heat-flow analysis. J. Aero/Sp. Sciences 26: 367-381. 1959.

36. Lardner, T. J. Biot's variational principle in heat conduction. AIAA Journ. 1: 196-206. 1963.

IX. APPENDIX A: VARIATIONAL PRINCIPLE FOR PROMPT NEUTRON KINETICS

In this appendix the variational principle used in this dissertation will be discussed and its validity for application to the reactor space-time problem will be verified.

The multigroup neutron diffusion equations, in the absence of any external sources, are given as

$$\vec{\nabla}\cdot D\,\vec{\nabla}\varphi + K\varphi + Q\varphi = V^{-1}\frac{\partial}{\partial t}\varphi \qquad (A.1)$$

where D is the diagonal matrix of group diffusion coefficients,

K is the lower triangular matrix whose diagonal elements are the negative of the group removal cross-sections and whose off diagonal elements are the group scattering cross-sections,

Q is the source matrix of fission neutrons

V^{-1} is the diagonal matrix of reciprocal group speeds,

φ is the column matrix of group fluxes.

In general the group diffusion coefficients are regionwise constants which leads to the continuity of current condition at the interface Γ_i

$$\left[D\,\vec{\nabla}\varphi\right]\Big|_{\Gamma_i-\epsilon} = \left[D\,\vec{\nabla}\varphi\right]\Big|_{\Gamma_i+\epsilon} \qquad (A.2)$$

The second boundary condition for Eq. A.1 is that the flux vanish on the external surface, Γ_a , of the reactor

$$\varphi(\Gamma_a) = 0 \qquad (A.3)$$

The equation adjoint to Eq. A.1 is found from the requirement

$$\int_{t_0}^{t_1} dt \int_V dr \left[\varphi^+ \mathcal{L} \varphi - \varphi \mathcal{L}^* \varphi^{+T} \right] = 0 \qquad \text{(A.4)}$$

where $\mathcal{L} = \vec{\nabla} \cdot D \vec{\nabla} + K + Q - V^{-1} \frac{\partial}{\partial t}$

and φ^{+T} is the column matrix of group adjoint fluxes. Proceeding with the operations indicated by Eq. A.4, the adjoint equation is found to be

$$\vec{\nabla} \cdot D \vec{\nabla} \varphi^{+T} + K^* \varphi^{+T} + Q^* \varphi^{+T} = -V^{-1} \frac{\partial}{\partial t} \varphi^{+T} \quad . \qquad \text{(A.5)}$$

The boundary conditions for the adjoint problem are similar to those for the flux,

$$\left[D \vec{\nabla} \varphi^{+T} \right]\Big|_{\Gamma_i - \epsilon} = \left[D \vec{\nabla} \varphi^{+T} \right]\Big|_{\Gamma_i + \epsilon} \qquad \text{(A.6)}$$

and

$$\varphi^+(\Gamma_a) = 0 \quad . \qquad \text{(A.7)}$$

For Eq. A.4 to be satisfied, a third condition is necessary

$$\int_{t_0}^{t_1} dt \int_V dr \, \frac{\partial}{\partial t} (\varphi^+ V^{-1} \varphi) = 0 \quad . \qquad \text{(A.8)}$$

This condition is referred to an "an adjoint boundary condition in time" by Kohler (28), and may be written as

$$\int_V dr \, (\varphi^+ V^{-1} \varphi) = \text{constant} \quad . \qquad \text{(A.9)}$$

The functional used in this study is a modification of the functional proposed by Kohler (28) in that the original formulation allowed for the use of mixed boundary conditions

on the outer boundary of the reactor, while the present formulation only permits the use of the Dirichlet boundary condition. While this restriction is of importance in describing small-reactors, it does not affect the results of this study.

The proposed variational principle is

$$L[\varphi^+,\varphi] = \int_{t_0}^{t_1} dt \int_V dr \left\{ \tfrac{1}{2}\left(\varphi^+ V^{-1}\frac{d\varphi}{dt} - \frac{d\varphi^+}{dt} V^{-1}\varphi\right) + \vec{\nabla}\varphi^+ \cdot D\vec{\nabla}\varphi - \varphi^+ H\varphi \right\}$$
$$+ \int_{t_0}^{t_1} dt \oint_{S_a} dS_a\, \varphi^+\varphi \quad - \tfrac{1}{2}\int_V dr \left\{ [\varphi^+ V^{-1}\varphi]|_{t_1} + [\varphi^+ V^{-1}\varphi]|_{t_0} \right\} \tag{A.10}$$

where $H = K + Q$. It is assumed that φ^+ and φ are contained in the admissible sets of functions which render L stationary. The variations $\delta\varphi^+$ in φ^+ and $\delta\varphi$ in φ are independent, thus the stationary condition of L can be written as

$$\delta L[\varphi^+,\varphi] = 0 = \delta L_1[\varphi^+,\varphi] + \delta L_2[\varphi^+,\varphi] \tag{A.11}$$

or

$$\delta L[\varphi^+,\varphi] = 0 = L_1'[\delta\varphi^+,\varphi] + L_2''[\varphi^+,\delta\varphi] \tag{A.12}$$

where δL_1 and δL_2 must vanish separately. The variation of φ^+ leads to the Euler-Lagrange equation for the flux, while the variation of φ leads to the Euler-Lagrange equation for the adjoint problem. The procedure to determine the Euler-Lagrange equations is the same for the two problems, therefore only the variation $\delta\varphi^+$ will be considered.

The variation of φ^+ gives

$$\delta L_1[\varphi^+,\varphi] = \int_{t_0}^{t_1} dt \int_V dr \left\{ \frac{1}{2}\left(\delta\varphi^+ V^{-1}\dot{\varphi} - \delta\dot{\varphi}^+ V^{-1}\varphi\right) + \vec{\nabla}\delta\varphi^+ \cdot D\vec{\nabla}\varphi - \delta\varphi^+ H\varphi \right\}$$
$$+ \int_{t_0}^{t_1} dt \oint_{\Gamma_a} dS_a\, \delta\varphi^+\varphi \quad - \frac{1}{2}\int_V dr \left\{ \left[\delta\varphi^+ V^{-1}\varphi\right]\Big|_{t_1} + \left[\delta\varphi^+ V^{-1}\varphi\right]\Big|_{t_0} \right\} \tag{A.13}$$

where $\dot{\varphi}^+$ indicates differentiation with respect to time. The term containing $\delta\dot{\varphi}^+$ is integrated by parts and combined with the second integral of Eq. A.13 to give

$$\int_{t_0}^{t_1} dt \int_V dr \left\{ -\frac{1}{2}\delta\dot{\varphi}^+ V^{-1}\varphi \right\} - \frac{1}{2}\int_V dr \left\{ \left[\delta\varphi^+ V^{-1}\varphi\right]\Big|_{t_1} + \left[\delta\varphi^+ V^{-1}\varphi\right]\Big|_{t_0} \right\}$$

$$= \int_V dr \left\{ -\left[\delta\varphi^+ V^{-1}\varphi\right]\Big|_{t_1} + \frac{1}{2}\int_{t_0}^{t_1} dt\; \delta\varphi^+ V^{-1}\dot{\varphi} \right\} . \tag{A.14}$$

The adjoint problem for dissipative processes is considered as a final value problem, thus $\delta\varphi^+|_{t_1}$ is zero.

The vector identity

$$\vec{\nabla}\cdot \delta\varphi^+ D\vec{\nabla}\varphi = \vec{\nabla}\delta\varphi^+ \cdot D\vec{\nabla}\varphi + \delta\varphi^+ \vec{\nabla}\cdot D\vec{\nabla}\varphi \tag{A.15}$$

and Gauss' theorem are applied regionwise to the surface of each ith region yielding the following result for the term involving gradient operation

$$\int_{t_0}^{t_1} dt \int_V dr \left\{ \vec{\nabla}\delta\varphi^+ \cdot D\vec{\nabla}\varphi = -\int_{t_0}^{t_1} dt \int_V dr\, \delta\varphi^+ (\vec{\nabla}\cdot D\vec{\nabla}\varphi) \right.$$
$$+ \sum_i \int_{t_0}^{t_1} dt \oint_{\Gamma_i} dS_i \left\{ \delta\varphi^+ D\vec{\nabla}\varphi\cdot\hat{n}_+ + \delta\varphi^+ D\vec{\nabla}\varphi\cdot\hat{n}_- \right\} . \tag{A.16}$$
$$\left. + \int_{t_0}^{t_1} dt \oint_{\Gamma_a} dS_a\; \delta\varphi^+ D\vec{\nabla}\varphi\cdot\hat{n}_a \right.$$

The second term arises from the fact that the application of Gauss' theorem at the inside surfaces results in the integra-

tion over each surface twice, with the outward unit normal in opposite direction at each surface Γ_i depending on the region under consideration. This term can also be written as

$$\sum_i \int_{t_0}^{t_1} dt \oint_{\Gamma_i} dS_i \left\{ \left([\delta\varphi^+ D\vec{\nabla}\vec{\varphi}]\Big|_{\Gamma_i+\epsilon} - [\delta\varphi^+ D\vec{\nabla}\vec{\varphi}]\Big|_{\Gamma_i-\epsilon} \right) \cdot \hat{n}_i \right\} \quad . \qquad (A.17)$$

Combining the results given by Eq. A.14 to Eq. A.17, the variation in φ^+ is given as

$$\delta L_1[\varphi^+,\varphi] = 0 = \int_{t_0}^{t_1} dt \int_V dr\ \delta\varphi^+ [V^{-1}\dot{\varphi} - \vec{\nabla}\cdot D\vec{\nabla}\vec{\varphi} - H\varphi] + \int_{t_0}^{t_1} dt \oint_{\Gamma_a} dS_a\ \delta\varphi^+ (D\vec{\nabla}\vec{\varphi}\cdot\hat{n}_a + \varphi)$$

$$+ \sum_i \int_{t_0}^{t_1} dt \oint_{\Gamma_i} dS_i \left\{ \left([\delta\varphi^+ D\vec{\nabla}\vec{\varphi}]\Big|_{\Gamma_i+\epsilon} - [\delta\varphi^+ D\vec{\nabla}\vec{\varphi}]\Big|_{\Gamma_i-\epsilon} \right) \cdot \hat{n}_i \right\} \quad . \qquad (A.18)$$

Since the variations in φ^+ are independent and arbitrary, the Euler-Lagrange equation for the flux, Eq. A.1, and its boundary conditions result from the proposed principle. This implies that for a given set of trial functions, the variational principle will select from that set those trial functions which best satisfy the Euler-Lagrange equation.

Two points of interest are to be noted. First, the exact extremals, that is the exact solution to the Euler-Lagrange equation, are not included in the sets of admissible trial functions, although they may be made up of some linear combination of the trial functions. If the selected trial functions render the functional stationary, they should be good approximations to the exact extremals.

A second point to be considered is that the stationarity

of the principle does not imply a maximum or minimum, but only a saddle-point. This is a restriction imposed by all principles of this type when applied to dissipative systems. Thus an estimate of the validity of the trial functions selected is to compare the asymptotic period of the exact solution, determined either by a finite difference calculation or by experiment, with the asymptotic period indicated by the approximate solution obtained with the trial functions.

X. APPENDIX B: DERIVATION OF THE EQUATIONS FOR THE GREEN'S FUNCTION MODES

In this appendix the derivation of the Green's function modes as introduced by Dougherty and Shen (12) and modified by Carter (14) will be reviewed.

The neutron diffusion equation, derived as one of the two Euler-Lagrange equations associated with the functional discussed in Appendix A, may be written as

$$L_r \varphi(r,t) - M\varphi(r,t) = V^{-1}\frac{\partial}{\partial t}\varphi(r,t) \qquad \text{(B.1)}$$

where L_r is a loss matrix and is given by

$$L_r = \vec{\nabla}\cdot D\vec{\nabla} - K$$

and M is the negative of the fission source matrix.

Following the scheme of Dougherty and Shen, Eq. B.1 is written in integral form as

$$\varphi(r,t) - \varphi_0(r) = \int_{t_0}^{t} dt' \Big\{ G(r,t;r',t')\, M(r',t')\, \varphi(r',t') \qquad \text{(B.2)}$$

The Green's function for Eq. B.2 is given by

$$\left(L_r - V^{-1}\frac{\partial}{\partial t}\right) G(r,t;r',t') = \delta(r-r')\,\delta(t-t') \qquad \text{(B.3)}$$

where $G(r,t;r',t')$ must satisfy the same boundary conditions that $\varphi(r,t)$ satisfy. To solve Eq. B.3, an iteration method is used with the approximation of zero order taken as the initial Green's function at time $t = t_0$. This Green's

function is given by

$$L_{ro}\, G(r,r') = \delta(r-r') \tag{B.4}$$

where L_{ro} is the steady state loss operator. The integrand of Eq. B.3 is approximated by

$$G(r,t;r',t')\, M(r',t')\, \varphi(r',t') \approx \sum_{i=1}^{N} C_i(t')\, G(r,r')\, M_o(r')\, \varphi_o(r')\, \Delta_i(r') \tag{B.5}$$

where $C_i(t')$ is the time coefficient in the ith region and

$$\Delta_i(r') \equiv \begin{cases} 1 & \text{in the ith region} \\ 0 & \text{elsewhere} \end{cases}$$

Substitution of Eq. B.5 into Eq. B.3 and integration of the resulting equation with respect to t gives

$$\varphi(r,t) = \varphi_o(r) + \int_{t_o}^{t} dt' \int_V dr' \left\{ \sum_{i=1}^{N} C_i(t')\, G_o(r,r')\, M_o(r')\, \varphi_o(r')\, \Delta_i(r') \right\}$$

$$= \varphi_o(r) + \sum_{i=1}^{N} \int_{t_o}^{t} dt' C_i(t') \int_V dr' \left\{ G_o(r,r')\, M_o(r')\, \varphi_o(r')\, \Delta_i(r') \right\} . \tag{B.6}$$

The flux is expressed as a finite sum of the space modes, $\psi_i(r)$, multiplied by the corresponding time coefficients $a_i(t)$, with the space modes given by

$$\psi_i(r) = \int_V dr' \left\{ G_o(r,r')\, M_o(r')\, \varphi_o(r')\, \Delta_i(r') \right. \tag{B.7}$$

and the time coefficients given by

$$a_i(t) = I + \int_{t_o}^{t} dt'\, C_i(t') \tag{B.8}$$

where I is the identity matrix.

A differential expression for the space functions is obtained by operating on both sides of Eq. B.7 by L_{ro} and integrating the resulting equation over r'. Utilization of

the definition of the Green's function given by Eq. B.4 leads to the following differential equation for the space modes

$$L_{ro}\,\psi_i(r) = M_o(r)\,\varphi_o(r)\,\Delta_i(r) \quad . \qquad (B.9)$$

Since $\sum_i L_{ro}\,\psi_i = L_{ro}\sum\psi_i = M_o\,\varphi_o(r)$, it is noted that the space modes must sum to the initial steady state flux.

The method of finding the adjoint space modes is similar to the method described for the flux modes, with the adjoint space modes given by

$$L_{ro}^{+}\,\psi_i^{+}(r) = M_o^{+}(r)\,\varphi_o^{+}(r)\,\Delta_i(r) \quad . \qquad (B.10)$$

The scheme discussed in the previous pages is applicable to any reactor system in which the various regions contain a fissionable material. If one of the regions does not contain a fissionable material, the right hand sides of Eq. B.9 and Eq. B.10 are zero. This is the expected result of applying the diffusion equation to a non-multiplying medium. Carter (14) investigated the time response of a coupled core reactor using the Green's function modes for the space trial functions, and found that it was necessary to have a source term for the mode in the coupling region to adequately describe any shape changes in the neutron flux. To this end the removal terms were divided in the manner given by

$$\Sigma_{ro} = \Sigma_r' + \Sigma_r'' \qquad (B.11)$$

where Σ_{ro} is the steady state value of the removal cross-section.

A two energy group problem without delayed neutrons is considered to illustrate the application of this method.

All fissions are assumed to occur in the thermal group with all fission neutrons entering the first group. The reactor model is a reflected slab reactor. Three regions will be considered, leading to a set of three trial functions. The left reflector is region one, the fuel region is region two, and the right reflector is region three. The matrices L_{ro} and M_o in regions one and three are given by

$$L_{ro} = \begin{bmatrix} \vec{\nabla}\cdot D_1\vec{\nabla} - \Sigma_{r1}' & 0 \\ 0 & \vec{\nabla}\cdot D_2\vec{\nabla} - \Sigma_{r2o} \end{bmatrix} \qquad \text{(B.12)}$$

$$M_o = \begin{bmatrix} 0 & \Sigma_{r1}'' \\ -\Sigma_{r1o} & 0 \end{bmatrix} . \qquad \text{(B.13)}$$

In region two the matrices L_{ro} and M_o have the form

$$L_{ro} = \begin{bmatrix} \vec{\nabla}\cdot D_1\vec{\nabla} - \Sigma_{r1o} & 0 \\ 0 & \nabla\cdot D_2\nabla - \Sigma_{r2o} \end{bmatrix} \qquad \text{(B.14)}$$

$$M_o = \begin{bmatrix} 0 & -\nu\Sigma_{f2} \\ -\Sigma_{r1o} & 0 \end{bmatrix} . \qquad \text{(B.15)}$$

The system of equations used to determine the space modes for the flux is given in Table B.1 and the equations for the adjoint space modes are given in Table B.2.

Table B.1. Space mode equations for problem in Appendix B

	Mode 1	Mode 2	Mode 3
Fast Group Modes			
Region 1	$\vec{\nabla}\cdot D_1\vec{\nabla}\psi_1 - \Sigma_{r1}'\psi_1 = \Sigma_{r1}''\varphi_{10}$ *	$\vec{\nabla}\cdot D_1\vec{\nabla}\psi_2 - \Sigma_{r1}'\psi_2 = 0$	$\vec{\nabla}\cdot D_1\vec{\nabla}\psi_3 - \Sigma_{r1}'\psi_3 = 0$
Region 2	$\vec{\nabla}\cdot D_2\vec{\nabla}\psi_1 - \Sigma_{r10}\psi_1 = 0$	$\vec{\nabla}\cdot D_1\vec{\nabla}\psi_2 - \Sigma_{r10}\psi_2 = -\nu\Sigma_{f2}\varphi_{20}$ **	$\vec{\nabla}\cdot D_1\vec{\nabla}\psi_3 - \Sigma_{r10}\psi_3 = 0$
Region 3	$\vec{\nabla}\cdot D_1\vec{\nabla}\psi_1 - \Sigma_{r1}'\psi_1 = 0$	$\vec{\nabla}\cdot D_1\vec{\nabla}\psi_2 - \Sigma_{r1}'\psi_2 = 0$	$\vec{\nabla}\cdot D_2\vec{\nabla}\psi_3 - \Sigma_{r1}'\psi_3 = \Sigma_{r1}''\varphi_{10}$
Thermal Group Modes			
Region 1	$\vec{\nabla}\cdot D_2\vec{\nabla}\psi_1 - \Sigma_{r20}\psi_1 = -\Sigma_{r10}\varphi_{10}$	$\vec{\nabla}\cdot D_2\vec{\nabla}\psi_2 - \Sigma_{r20}\psi_2 = 0$	$\vec{\nabla}\cdot D_2\vec{\nabla}\psi_3 - \Sigma_{r20}\psi_3 = 0$
Region 2	$\vec{\nabla}\cdot D_2\vec{\nabla}\psi_1 - \Sigma_{r20}\psi_1 = 0$	$\vec{\nabla}\cdot D_2\vec{\nabla}\psi_2 - \Sigma_{r20}\psi_2 = -\Sigma_{r10}\varphi_{10}$	$\vec{\nabla}\cdot D_2\vec{\nabla}\psi_3 - \Sigma_{r20}\psi_3 = 0$
Region 3	$\vec{\nabla}\cdot D_2\vec{\nabla}\psi_1 - \Sigma_{r20}\psi_1 = 0$	$\vec{\nabla}\cdot D_2\vec{\nabla}\psi_2 - \Sigma_{r20}\psi_2 = 0$	$\vec{\nabla}\cdot D_2\vec{\nabla}\psi_3 - \Sigma_{r20}\psi_3 = -\Sigma_{r10}\varphi_{10}$

* φ_{10} is the steady state flux distribution for the fast group
** φ_{20} is the steady state flux distribution for the thermal group

Table B.2. Adjoint space mode equations for problem in Appendix B

	Mode 1	Mode 2	Mode 3
Fast Group Adjoint Modes			
Region 1	$\vec{\nabla}\cdot D_1\vec{\nabla}\psi_1^+ - \Sigma_{r10}\psi_1^+ = -\Sigma_{r10}\varphi_{20}^+$ *	$\vec{\nabla}\cdot D_1\vec{\nabla}\psi_2^+ - \Sigma_{r10}\psi_2^+ = 0$	$\vec{\nabla}\cdot D_1\vec{\nabla}\psi_3^+ - \Sigma_{r10}\psi_3^+ = 0$
Region 2	$\vec{\nabla}\cdot D_1\vec{\nabla}\psi_1^+ - \Sigma_{r10}\psi_1^+ = 0$	$\vec{\nabla}\cdot D_1\vec{\nabla}\psi_2^+ - \Sigma_{r10}\psi_2^+ = -\Sigma_{r20}\varphi_{20}^+$	$\vec{\nabla}\cdot D_1\vec{\nabla}\psi_3^+ - \Sigma_{r10}\psi_3^+ = 0$
Region 3	$\vec{\nabla}\cdot D_1\vec{\nabla}\psi_1^+ - \Sigma_{r10}\psi_1^+ = 0$	$\vec{\nabla}\cdot D_1\vec{\nabla}\psi_2^+ - \Sigma_{r10}\psi_2^+ = 0$	$\vec{\nabla}\cdot D_1\vec{\nabla}\psi_3^+ - \Sigma_{r10}\psi_3^+ = -\Sigma_{r1a}\varphi_{20}^+$
Thermal Group Adjoint Modes			
Region 1	$\vec{\nabla}\cdot D_2\vec{\nabla}\psi_1^+ - \Sigma_{r2}'\psi_1^+ = \Sigma_{r2}''\varphi_{20}^+$	$\vec{\nabla}\cdot D_2\vec{\nabla}\psi_2^+ - \Sigma_{r2}'\psi_2^+ = 0$	$\vec{\nabla}\cdot D_1\vec{\nabla}\psi_3^+ - \Sigma_{r2}'\psi_3^+ = 0$
Region 2	$\vec{\nabla}\cdot D_2\vec{\nabla}\psi_1^+ - \Sigma_{r20}\psi_1^+ = 0$	$\vec{\nabla}\cdot D_2\vec{\nabla}\psi_2^+ - \Sigma_{r20}\psi_2^+ = -\nu\Sigma_{f2}\varphi_{10}^+$ **	$\vec{\nabla}\cdot D_1\vec{\nabla}\psi_3^+ - \Sigma_{r20}\psi_3^+ = 0$
Region 3	$\vec{\nabla}\cdot D_2\vec{\nabla}\psi_1^+ - \Sigma_{r2}'\psi_1^+ = 0$	$\vec{\nabla}\cdot D_2\vec{\nabla}\psi_2^+ - \Sigma_{r2}'\psi_2^+ = 0$	$\vec{\nabla}\cdot D_2\vec{\nabla}\psi_3^+ - \Sigma_{r2}'\psi_3^+ = \Sigma_{r2}''\varphi_{20}^+$

* φ_{20}^+ is the steady state adjoint flux distribution for the thermal group
** φ_{10}^+ is the steady state adjoint flux distribution for the fast group